Energy, exergy, economic and exergoeconomic (4E) multicriteria analysis of an industrial waste heat valorization system through district heating

Jaume Fitó, Julien Ramousse, Sacha Hodencq, Frédéric Wurtz

Energy, exergy, economic and exergoeconomic (4E) multicriteria analysis of an industrial waste heat valorization system through district heating

Jaume Fitó[a], Julien Ramousse[a,], Sacha Hodencq[b], Frédéric Wurtz[b]*

[a] *Laboratoire Optimisation de la Conception et Ingénierie de l'Environnement (LOCIE), CNRS UMR 5271 – Université Savoie Mont Blanc, Polytech Annecy-Chambéry, Campus Scientifique, Savoie Technolac, 73376 Le Bourget-Du-Lac Cedex, France*

[b] *Univ. Grenoble Alpes, CNRS, Grenoble INP[*], G2Elab, F-38000 Grenoble, France*

** Corresponding author: J. Ramousse.*

Abstract

The purpose of this article is to determine the multicriteria-optimal design of an industrial waste heat recovery system for district heating in Grenoble (France). Energy, exergy and cost flow balances were applied unit by unit allowing to assess the process performance based on two innovative methods. First, the performance assessment includes all units involved in the heat valorization process, not only focusing on the recovery system. Second, the yearly management of energy flows was optimized through mixed-integer linear programming, anticipating fluctuations in residential demands and waste heat availability. This multicriteria analysis with a systemic-anticipative approach allowed to select the appropriate inlet temperature and storage capacity. It was found that the most promising inlet temperature and heat storage capacity are 35 °C and 30 MWh, respectively. With this design, the system recovers 41% of industrial waste heat, covers 48% of residential needs, has an estimated net present value of 11.7 million euros over 20 years, and reduces the district's overall exergy destruction and exergy destruction costs by 20% (4.2 GWh/year) and 9% (286 k€/year), respectively. Remarkably, none of the mono-criterion analyses prioritized this design. Therefore, the multicriteria analysis with systemic-anticipative approach was of utmost importance for detecting the most promising solution.

Keywords: District heating, Waste heat recovery, Exergy, Exergo-economics, 4E Analysis.

Highlights

- Systemic approach englobing the industry, recovery system and district network.
- Anticipative optimization of yearly energy management depending on availability.
- Promising storage capacity and inlet temperature determined by overall indicators.
- Distinct optimum for each criterion, leading to five dual-criteria Pareto fronts.
- Most suitable multi-criteria design not detected by mono-criteria assessments.

[*] Institute of Engineering Univ. Grenoble Alpes

Nomenclature

Names and Variables		***Subscripts and Superscripts***	
C	Capital cost (k€)	BEP	Breakeven Point
$\dot{C}$	Cost flow (k€/year)	C	Carnot cycle
c	Specific exergy cost (k€/GW_{ex})	ch	Chemical
CF	Coverage Factor (%)	chrg	Heat charge of the thermal storage unit
COM	Costs of Operation and Maintenance (k€)	CI	Related to capital investment
COP	Coefficient Of Performance (GW_{th}/GW_{el})	cooling	Magnet's cooling process
E	Exergy (GWh)	D	Destruction
$\dot{E}$	Exergy flow (GW)	dchg	Heat discharge of the thermal storage unit
ECON	Economic criterion	DHN	District Heating Network
ENER	Energetic criterion	DISS	Dissipation
EXER	Exergetic criterion	elec	Electrical
EXEC	Exergo-economic criterion	ex	Exergetic
f	Exergoeconomic factor (k€/k€)	exo	Exogenous
i	Effective rate of return (%/year)	F	Fuel
n	Economic lifespan of the equipment (years)	f	Final
NPV	Net Present Value (k€)	OM	Related to operation and maintenance
Q	Heat (kWh, MWh or GWh)	out	Outlet
$\dot{Q}$	Thermal power (GW)	Q	Heat
PEC	Purchased Equipment Cost (k€)	GLOB	Overall
r	Relative cost difference (%)	HP	Heat pump
RACF	Recovery And Coverage Factor	HS	Heat supplier
RF	Recovery Factor	in	Inlet
T	Temperature (K)	ini	Initial
T_0	Temperature of the dead state (K)	L	Losses
t	Time (h)	LNCMI	Laboratoire National des Champs Magnétiques Intenses
TCI	Total Capital Investment (k€)	magnets	LNCMI's high-intensity magnets
U	Internal energy (GWh)	max	Maximal
$\dot{W}$	Work (electric) power (GW)	min	Minimal
$\dot{Z}$	Annuity (k€/year)	mono	Mono-criterion
		multi	Multi-criterion
Greek Symbols		out	Outlet
Δt	Time step (h)	P	Product
ε	Exergy efficiency (%)	piping	Overall pipeline layout
ξ	Electricity-to-heat conversion ratio (GW_{th}/GW_{el})	q	Related to heat
θ	Exergy factor	REF	Reference scenario
ψ	Relative performance amongst all solutions	SST	Network sub-stations
χ	Value of the performance indicator	TES	Thermal Energy Storage
		u	Related to internal energy
		use	Useful exergy destruction
		wh	Waste heat
		WHRS	Waste Heat Recovery System

1. Introduction

Space heating represents a non-negligible amount of end-user energy consumption, especially in the urban residential sector, where district heating is more and more commonly used [1]. In particular, low-temperature district heating has been identified by the International Energy Agency as a key enabling technology to increase the integration of renewable sources, including waste energy [2]. Recovery of industrial waste heat and its integration in district heating are more and more encouraged globally [3]. For instance, McKenna et al [4] evaluated around 90 % of energy-intensive sectors in UK and estimated a potential of 10 TWh to 20 TWh for technically feasible waste heat recovery. Svensson et al [5,6] evaluated the trade-off between using waste heat, sometimes called excess heat, internally for the industrial process itself, or externally for district heating. They concluded that both of them are profitable strategies, and that external use, i.e. industry/district network cooperation, tends to give lower CO_2 emissions than internal use. Miró et al [7] identified some aspects that need further development in the integration of industrial waste heat into district heating. Such aspects included (but not limited to) a lack of large scope and high spatial resolution in the analyses, and an apparent reluctance by some industrial actors to publish useful data about their waste streams.

Based on this information, one could say that waste heat is an abundant source with integration opportunities, but it is under-documented and under-utilized for the moment [8]. New research contributions to the field can directly solve the first issue, and help solving the second one. Investigations based on mixed electric-thermal models are emerging in countries and areas where heat districts are historically developed, like eastern and northern Europe [9]. Such kinds of projects can benefit from a diversity of criteria, because they involve energy flows of different types and qualities. Thus, conventional techno-economic analyses may not suffice to identify the best opportunities. Energy analysis alone is also insufficient to provide information on the quality of energy streams in a system [10]. Fortunately, thermodynamics has yielded in the recent decades some applicable and easily interpretable criteria to further improve energy systems.

One of them is exergy. It gives information on how to optimally transform energy [11], and it can either confirm or be in contrast with energy-based analysis [12]. The interest of exergy is claimed by many specialists [11,13–15], not only for engineering but also in energy policy making [16]. Besides, exergy destruction is an indicator that does not encounter a direct equivalent in first-law analyses. That makes it interesting because it can suggest unique alternative solutions. Exergy analysis has been applied in several studies on district heating and waste heat utilization. For instance, Bühler et al [17] applied exergy analysis on the Danish industry sector to improve its efficiency and identify the potential for waste heat recovery within industrial processes. Solheimslid et al [18] performed the first-law and second-law analyses of a Norwegian combined heat and power facility driven by municipal waste incineration. Wang et al [19] sustained exergy as a crucial optimization criterion for heat pumps that aim to recover industrial waste heat for utilization in district heating. It has also been used successfully as an objective function in control algorithms for district energy networks [10]. The other interesting criterion is exergoeconomics. Exergoeconomics is defended by thermodynamic experts as the proper way of accounting monetarily for thermodynamic inefficiencies within energy systems [11,14]. Exergoeconomics are becoming relevant for district energy networks analysis. For instance, Baldvinsson and Nakata [20] applied the LowEx and SPECO methods on a local source-based district heating system in Japan. Their study was carried out from a single user perspective. Zhang et al [21] developed a novel cost-pricing model based on exergy analysis, for a more efficient evaluation of the district heating market. Čož et al [22] used the exergetic product cost as objective function to optimize the diameter and insulation thickness of a 1000 m-long

pipeline for district cooling. Although not abundant, some studies exist on the exergoeconomic analysis of heat pumps at a district scale, but many of them focus on geothermal technologies [23,24].

The above comments justify the need and interest of applying exergy and exergoeconomic analyses in design projects. When combined with conventional energy, economic or environmental analyses, they lead to a 3E or 4E multicriteria analysis. These analyses excel in finding better ways to manage energy resources, especially if each criterion suggest a non-redundant solution with respect to the others. Consequently, it is no surprise that 3E and 4E multicriteria analyses are becoming a common procedure in assessing renewable energy integrations, energy recovery within conventional processes, or waste-to-energy systems [25–27]. For instance, Liu et al [28] applied multicriteria analysis to assess waste heat recovery within a syngas process with carbon capture and storage. Ameri et al [29] applied 4E analysis with genetic algorithm to optimize a large steam power plant, increasing its energy and exergy efficiencies by 9.7% and 16.8%. Wang et al [30] performed a 4E analysis on a distributed generation solar-assisted combined cooling, heating and power gas turbine system, achieving 41% less carbon emissions with respect to the non-solar system. Further, their off-design analysis demonstrated that energy and exergy efficiencies alone would not have sufficed to prove the advantages of the solar integration. This means that both the exergoeconomic and the environmental criteria were relevant. Elbar et al [31] applied 4E analysis for the integration of a solar still with photovoltaic panels. Multicriteria analyses have also been used to assess chemical engineering processes. For example, Wang et al [32] combined thermodynamic, thermo-economic and life cycle environmental analyses to assess ketone ammoximation production. Meng et al [33] selected the best design of a distillation-pervaporation process based on energy, economic and environmental evaluations.

Multicriteria analyses are also being applied to district heating projects. For example, Ajah et al [34] studied the technical, economic, institutional and environmental feasibilities of a robust industrial waste heat-driven district heating system including recycle of exhaust residential heat after end-user utilization. Baldvinsson and Nakata [20] considered in their study exergy efficiency, monetary costs and exergoeconomic costs to compare the current heat supply system paradigm in Japan with an innovative one integrating several renewable and waste sources. Ghafghazi et al [35] evaluated different types of district heating options through multicriteria analysis. Their study did not consider industrial waste heat recovery, but it did include other interesting renewable options such as biomass, geothermal heat exchange, and sewer heat recovery. More recently, Dorotić et al [36] performed a multi-objective optimization of district heating systems through economic, environmental and exergetic indicators. Their study yielded a 3-D Pareto front that shows the need for compromise between the three criteria, since each one suggested a unique optimal solution.

Further, the search for new approaches in district heating with industrial waste heat recovery is still active. Dénarié et al [37] proposed an assessment methodology based on multicriteria decision analysis in order to cope with uncertainties related to input data quality in these kinds of projects. They exemplified the use of their methodology with a real study case in Milano, Italy. Wang et al [38] developed a multicriteria decision support framework for district heating based on combined heat and power systems. Fang et al [39] analyzed key issues in district heating using low-grade industrial heat, and proposed an approach based on “tangency technology” to facilitate integration of multiple waste heat sources. Recently, Woolley et al [40] proposed a 4-step systematic approach including exergy balances, in order to assess industrial waste heat recovery opportunities. They suggested the approach as a support tool for industrial decision-makers. Some of the recent studies consider mixed-integer linear programming for the optimization, like the work of Oluleye et al [41], which uses it for integrating thermodynamic cycles in process sites with the purpose of waste heat exploitation.

Many studies on decision aiding for district heating focus on a single decision-maker or, at most, a small group of decision-makers from a same organization. However, district heating projects with several heat sources can involve different stakeholders, that would prefer different optimal designs. Ghafghazi et al [35] demonstrated with their study that communication between those stakeholders can lead to consensus and change the final design significantly. There do not seem to be abundant studies in literature that evaluate industrial waste heat recovery for district heating through multicriteria analysis assuming perfect consensus between the stakeholders. Besides, not many multicriteria studies on industrial waste heat recovery for district heating utilization use the exergo-economic criterion.

Our article contributes to that niche. We analyze the integration of industrial waste heat in a district heating network by approaching the industrial process, the heat recovery system, the district network and its auxiliary facilities all as one same system. The aim of this systemic approach is to determine the most suitable inlet temperature and thermal storage capacity of the recovery system. We apply local balances, but define overall performance indicators that involve all parties affected by the project, and assume perfect consensus between the stakeholders. In addition, we support our yearly simulation with a mixed-integer linear programming tool that allows to anticipate the district's needs and the waste heat's availability. As the mono-criterion and multi-criteria results show, each one of the four criteria (energy, exergy, economy and exergoeconomics) suggests a different optimal solution, and so does the multi-criteria assessment. We also point out that a decision based only on the recovery system's performance would have led to another design. Therefore, both the multicriteria analysis and our systemic approach were necessary to identify the most promising solution.

2. Materials and method

The selected method consists in applying 4E analyses (energy, exergy, economic and exergoeconomic) on different scenarios where yearly management of energy flows has been previously optimized by means of Mixed-Integer Linear Programming (MILP). The MILP-assisted optimization of the system's yearly operation consisted in determining the best management of energy flows depending on the objective. The aim of the 4E analyses is to determine the most suitable inlet temperature and storage capacity of the waste heat recovery system. Although the design parameters are local, each scenario has been approached englobing all units involved in the heat valorization process.

2.1. System description and modelling tool

Figure 1 shows the exergo-diagram of the system. The position of each arrow within the y-axis indicates the quality (i.e. exergy) of that energy stream. Continuous lines represent the existing system. Dashed lines represent the prospective system and its different possible temperature levels.

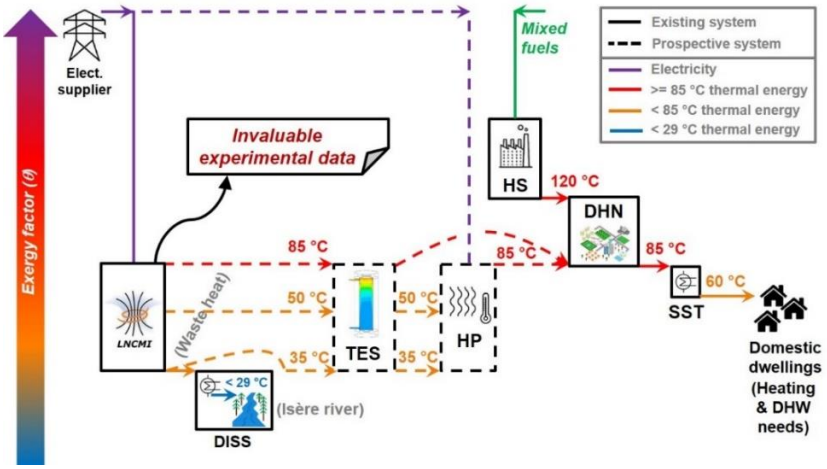

Figure 1. Exergo-diagram of the case study with the existing and prospective units.

The current scenario (solid lines in Fig. 1) is made up of the following units, described by the associated abbreviations:

- LNCMI: LNCMI is the French national laboratory for high-intensity magnetic fields in Grenoble (*Laboratoire National des Champs Magnétiques Intenses*). It provides high magnetic fields for worldwide researchers. Their electro-intensive activities generate important amounts of low-temperature waste heat.
- DISS: This unit is used to dissipate LNCMI's waste heat in a nearby river (Isère).
- DHN: The local District Heating Network in the proximities of the LNCMI, provide residential users with low-temperature heat.
- SST: The substations associated to the DHN provide residential users with low-temperature heat for space heating and Domestic Hot Water production.
- HS: A nearby Heat Supplier that currently covers all the needs of the DHN.

The studied scenario aims at recovering LNCMI's waste heat for utilization in the DHN. This would be done through a Waste Heat Recovery System (WHRS) represented by dashed lines in fig. 1 and made up of:

- HP: An electrically-driven mechanical Heat Pump has to be used to upgrade heat's temperature whenever necessary. Its inlet temperature depends on the scenario, but the outlet temperature has to reach 85 ˚C for injecting heat into the DHN. Mechanical heat pumps are a mature technology whose technical details are available to the general public.
- TES: A Thermal Energy Storage unit is additionally considered to compensate for short-term temporal mismatch and absorb the highest power peaks of waste heat. Well-documented studies [42] have stated that this component allows to overcome the intermittence and distance between the waste heat source and the application site. Stratified thermal storage and thermocline modelling are interesting research topics in the recent years [43]. The TES considered in this study is a non-pressurized thermocline storage containing liquid water.

The sections below describe the 4E (energy, exergy, economic and exergoeconomic) models developed for multi-criteria analysis, and the preliminary approach to determine the most suitable design for the heat recovery system.

These analyses were applied after optimizing the yearly management of energy flows through mixed-integer linear programming. The tool used in the present article is an open-source tool called OMEGAlpes [44].

2.2. Input data

Figure 2a shows the power tranches of both the LNCMI and the DHN. Figure 2b shows the model hourly profile used for the LNCMI's yearly electricity consumption. It has been constructed from different fragments of several operating years, aiming at defining a representative operation profile. Therefore, each and every point is a real datum, but the profile does not correspond integrally with any operating year. The hourly profile of residential heat demand at the DHN is protected by confidentiality clauses against diffusion to the general public. This critical issue is stated by Miró et al [7] in their conclusions: industrial actors do not usually publish their waste streams characteristics, which could facilitate very accurate analyses.

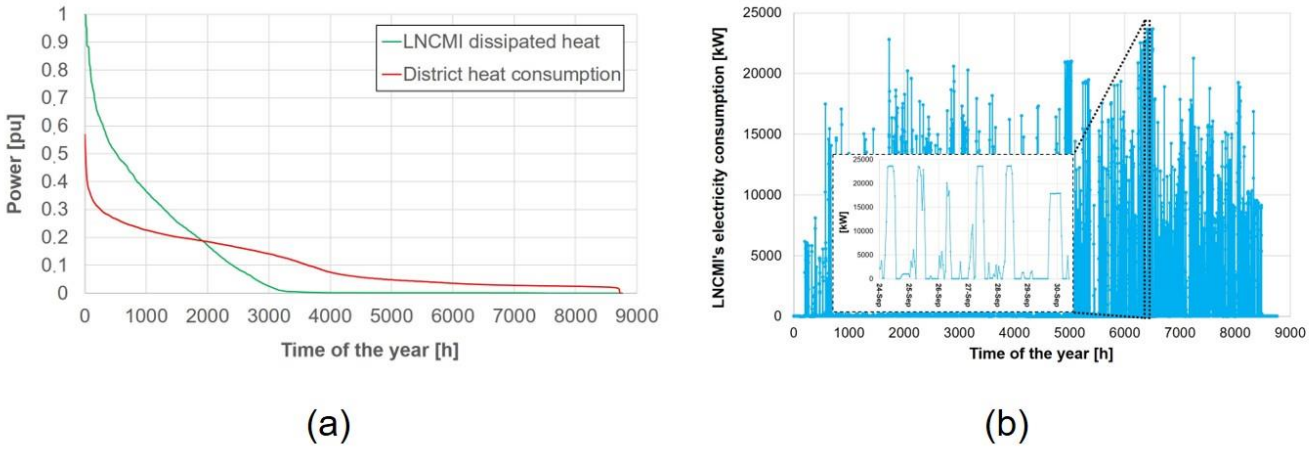

Figure 2. a) LNCMI's and Heat Supplier's power tranches; b) Estimated LNCMI's electricity consumption profile.

Table 1 contains the values used for the 4E model's input parameters, classified with respect to the model they are related to. Parameters that have a range of values are optimization parameters and their value was changed from one scenario to another. In addition, some other parameters varied depending on the waste heat's temperature. It is the case of electricity-to-heat conversion ratio within the LNCMI (ξ), or the heat pump's COP, for instance.

Table 1. Input parameters of the simulations.

Model	Magnitude	Value(s) or limit(s)	Units	Reference
Energy	Initial time of simulation (t_{ini})	0	h	[12]
	Final time of simulation (t_f)	8760	h	[12]
	Time step (Δt)	1	h	[12]
	Electricity-to-heat conversion ratio with waste heat at 35 °C ($\xi\,(35\,°C)$)	0.85	kW_{th} / kW_{el}	[12]
	Electricity-to-heat conversion ratio with waste heat at 50 °C ($\xi\,(50\,°C)$)	0.80	kW_{th} / kW_{el}	[12]
	Electricity-to-heat conversion ratio with waste heat at 85 °C ($\xi\,(85\,°C)$)	0.70	kW_{th} / kW_{el}	[12]
	Heat pump's performance $\left(COP_{HP}(T_{HP}^{in} = 35\,°C)\right)$	3	kW_{th} / kW_{el}	[12]
	Heat pump's performance $\left(COP_{HP}(T_{HP}^{in} = 50\,°C)\right)$	4.29	kW_{th} / kW_{el}	[12]
	Heat pump's maximum inlet power $\left(\dot{W}_{HP}^{el,max}(T_{HP}^{in} = 35\,°C)\right)$	1260	kW_{el}	[12]
	Heat pump's maximum inlet power $\left(\dot{W}_{HP}^{el,max}(T_{HP}^{in} = 50\,°C)\right)$	881	kW_{el}	[12]
	Thermal storage's maximum capacity (U_{TES}^{max})	[0, 10, 20, 30, 40]	MWh	[12]
	Thermal storage's maximum charging power ($\dot{Q}_{TES}^{in,max}$)	$= U_{TES}^{max}/3$	MW	[12]
	Thermal storage's maximum discharging power ($\dot{Q}_{TES}^{out,max}$)	$= U_{TES}^{max}/3$	MW	[12]
Exergy	Dead state temperature (T_0)	8	°C	[12]
	Heat supply unit's exergy efficiency (ε_{HS})	0.4	kW_{ex} / kW_{ex}	[12]

	Temperature difference for magnets' cooling ($\Delta T_{\text{cooling}}$)	60	˚C	[45]
	Waste heat temperature ($\mathrm{T_{wh}}$)	[35, 50, 85]	˚C	[12]
	Heat pump's inlet temperature ($\mathrm{T_{HP}^{in}}$)	[35, 50]	˚C	[12]
	Heat pump's outlet temperature ($\mathrm{T_{HP}^{out}}$)	85	˚C	[12]
	Heat supply unit's service temperature ($T_{HS}^{q,out}$)	120	˚C	[12]
	End-users heat temperature	60	˚C	[12]
Economy	Heat pump's purchase equipment cost $\left(\mathrm{PEC_{HP}}\left(\mathrm{T_{HP}^{q,in}} = 35\ ^{\circ}\mathrm{C}\right)\right)$	810	k€	[36]
	Heat pump's purchase equipment cost $\left(\mathrm{PEC_{HP}}\left(\mathrm{T_{HP}^{q,in}} = 50\ ^{\circ}\mathrm{C}\right)\right)$	526	k€	[36]
	Coefficient of thermal storage's purchase cost ($\mathrm{c_{TES}^{PEC}}$)	90	k€/MWh-capacity	[46]
	Coefficient of piping costs ($\mathrm{c_k^{pipe}}$)	0.7	k€/(k€ of PEC)	[11]
	Coefficient of operation and maintenance costs ($\mathrm{c_k^{OM}}$)	0.1	k€/(k€ of TCI)	[11]
	Economic observation period (n)	20	years	[11]
	Effective rate of return (i)	0.06	-	[11]
	Specific buy cost of electricity from the grid ($\mathrm{c^{elec}}$)	120	€/MWh$_{\text{elec}}$	[47]
	Specific sell cost of heat for residential end-users ($\mathrm{c_{SST}^{q,out}}$)	80	€/MWh$_{\text{heat}}$	[47]

2.3. Governing equations and main hypotheses

The simulations were based on applying a thermodynamic analysis with energy, exergy and their corresponding cost flow balances unit by unit. The four models are internally correlated. The exergy and economy models are built on the energy model, and the exergoeconomic model is built on the exergy and economy model. Therefore, many of the energetic and economic parameters are shared between the models. A change in any energy parameter has an impact on the rest of the models. Economic parameters, especially the costs of energy streams, also influence exergoeconomic results.

ENER: Energy model

The energy model relies on energy balance applied to each unit of the recovery system. The following hypotheses were used in the energy model:

- Potential and kinetic energy are neglected.
- Temperature levels of the units remain constant throughout the year.
- Pressure, temperature and heat losses across the pipelines are neglected.
- Perfect stratification is assumed in the thermal storage unit.
- The initial and final state of charge of the thermal energy storage are the same.
- Heat losses across the different components of the heat pump are neglected.
- The heat production process by the heat supplier has a constant exergetic efficiency (ε_{HS}).

In its general form (eq. 1), a non-steady energy balance on a unit at each time step (Δt) accounts for heat inlets $\left(\dot{Q}^{in}\right)$, heat outlets ($\dot{Q}^{out}$), power inlets ($\dot{W}^{in}$), power outlets ($\dot{W}^{out}$) and energy accumulations (ΔU) within the unit. Refer to Table A.1 in Appendix A for concretized unit-by-unit energy balances. Most of the units in this study case have no accumulation within them (i.e. $\Delta U = 0$), except for the thermal storage unit.

$$\Delta t \cdot \sum\left(\dot{Q}^{in} + \dot{W}^{in}\right) = \Delta t \cdot \sum\left(\dot{Q}^{out} + \dot{W}^{out}\right) + \Delta U \tag{1}$$

EXER: Exergy model

Similarly to the energy model, the exergy model results from exergy balances applied to each of the unit. The following hypotheses were used in the exergy model:

- Potential and kinetic exergy are neglected.
- The heat production process by the heat supplier has a constant exergetic efficiency (ε_{HS}).

The non-steady exergy balance (eq. 2) accounts for the abovementioned power inlets and outlets, the exergy inlets ($\dot{E}^{in}$) and outlets ($\dot{E}^{out}$), exergy destruction ($\dot{E}^{D}$) and exergy accumulation (ΔE^{u}) within the unit. Refer to Table A.2 in Appendix A for concretized unit-by-unit exergy balances. The accumulation term is only considered for the thermal storage unit, like in the energy model. The exergy of thermal flows ($\dot{E}^{q}$) was determined as a function of their temperature (eq. 2.a). The dead state temperature (T_0) was kept constant, for thermodynamic consistency [48]. Electric power can be included directly in the balance because its exergy factor is equal to 1.

$$\Delta t \cdot \sum\left(\dot{E}^{in} + \dot{W}^{in}\right) = \Delta t \cdot \left[\sum\left(\dot{E}^{out} + \dot{W}^{out}\right) + \dot{E}^{D}\right] + \Delta E^{u} \tag{2}$$

$$\text{With } \dot{E}^{q} = \dot{Q} \cdot \left(1 - \frac{T_0}{T_q}\right) \tag{2.a}$$

ECON: Economic model

The economic model aims to evaluate profitability of the project and the product's final price. The economic model is sustained on the following hypotheses:

- The analysis is done with 'constant dollars' (i.e. no inflation). This approach is best suited for analyses involving economic periods longer than 10 years [11].
- Prices of fuels and products are not subject to escalation or changes in the contracts.
- Capital investments on all existing equipment of the LNCMI, the HS and the DHN owner are completely recovered. Thus, the only capital investment to assess relates to the WHRS.
- The purchased equipment cost and the cost of piping are the only contributions to the fixed capital investments. Other contributions (offsite costs, indirect costs…) are dismissed.
- The two potential investors (i.e. the LNCMI and the HS) form a joint Consortium. Both agree to the price of LNCMI's waste heat and respect it for the whole economic life of the equipment. All profits obtained through the WHRS are mutualized proportionally to each one's initial investment.

Heat sold by the DHN to the residential end-users remains at the same price (its current price) throughout the equipment's economic life.

The cost flow balance (eq. 3) states that the yearly product sales revenues ($\dot{C}^{P}$) should compensate the fuel costs ($\dot{C}^{F}$) and amortize the annuities $\left(\dot{Z}\right)$ related to capital expenditures. Refer to Table A.3 in Appendix A for concretized unit-by-unit formulations of the cost flow balance. In this study, the cost flow balance was applied downstream in most cases, in order to determine product costs from known fuel costs and annuities. The only 3 exceptions took place at the reference scenario, in the balances on the SST, the DHN and the HS. Those balances were applied upstream, starting at the SST with a known sell price for the heat, fixed by a contract with the residential end-users. The aim of those upstream balances was to determine the specific fuel and product costs, both energetic and exergetic, of the HS's combustion process. Those two last costs were kept as input parameters for the rest of the scenarios.

$$\sum \dot{C}^F + \dot{Z} = \sum \dot{C}^P \quad (3)$$

Two types of annuities were assessed (eq. 4). One type ($\dot{Z}^{CI}$) is related to the Total Capital Investment (TCI), which is the sum (eq. 4.a) of the Purchase Equipment Cost (PEC) and the costs of piping (c^{pipe}). The costs of piping were relevant to this case study because district heating requires long pipelines with relatively big diameters. The other type of annuity ($\dot{Z}^{OM}$) is related to the Costs of Operation and Maintenance (COM), which were assumed as a fraction (c^{OM}) of the total capital investment (eq. 4.b). All capital costs were transformed into annuities through The Capital Recovery Factor (*CRF*, eq. 4.c), which accounts for the economic observation period (*n*) and the interest rate (*i*).

$$\dot{Z} = \dot{Z}^{CI} + \dot{Z}^{OM} = (TCI \cdot COM) \cdot CRF \quad (4)$$

$$\text{With } TCI = PEC \cdot (1 + c^{pipe}) \quad (4.a)$$

$$COM = c^{OM} \cdot TCI \quad (4.b)$$

$$CRF = \frac{i \cdot (1+i)^n}{(1+i)^n - 1} \quad (4.c)$$

EXEC: Exergo-economic model

Exergo-economics claims that exergy is the only rational basis for assigning monetary costs to the interactions of a system with its surroundings and to the sources of thermodynamic inefficiencies within it [13]. The exergoeconomic approach in this study followed the SPecific Exergy COsting method (SPECO) [14]. After the exergy and economic analyses have been performed, the application of this method is almost straightforward. The average specific exergy costs of the inlets (c^F) and outlets (c^P) of each unit were determined through the Fuel principle (eq. 5) and the Product principle (eq. 6), respectively.

$$c^F = C^F / E^F \quad (5)$$

$$c^P = C^P / E^P \quad (6)$$

2.4. Performance indicators

Given the multi-temporal architecture of the model, performance indicators are best assessed by integration of the hourly profiles throughout the year. Three energy-based indicators were used in this study. The Recovery Factor (*RF*, eq. 7) is the ratio between the total yearly intake of waste heat (Q^{in}_{WHRS}) and the total waste heat available (Q^{out}_{LNMCI}). The Coverage Factor (*CF*, eq. 8) is the ratio between the total heat injected to the district network (Q^{out}_{WHRS}) and the total residential demands (Q^{out}_{DHN}). The Recovery And Coverage Factor (*RACF*, eq. 9) looks for balance between heat recovery and residential coverage.

$$RF = \frac{Q^{in}_{WHRS}}{Q^{out}_{LNMCI}} = \frac{\sum_{t=t_{ini}}^{t=t_f} \dot{Q}^{in}_{WHRS} \cdot \Delta t}{\sum_{t=t_{ini}}^{t=t_f} \dot{Q}^{out}_{LNMCI} \cdot \Delta t} \quad (7)$$

$$CF = \frac{Q^{out}_{WHRS}}{Q^{out}_{DHN}} = \frac{\sum_{t=t_{ini}}^{t=t_f} \dot{Q}^{out}_{WHRS} \cdot \Delta t}{\sum_{t=t_{ini}}^{t=t_f} \dot{Q}^{out}_{DHN} \cdot \Delta t} \quad (8)$$

$$RACF = RF \cdot CF \quad (9)$$

The exergy indicator is the district's overall efficiency (ε_{GLOB}). To determine it, all exergy destructions (E^{D}_{GLOB}) and the district's exergy inlets (E^{in}_{GLOB}) were taken into account (eq. 10). This includes the LNCMI's process, the heat dissipation, the thermal storage, the heat pump, the Heat Supplier's process, the district network and the residential dwellings (eq. 11). The exergy inlets of the overall district (eq. 12) are the LNCMI's electricity consumption ($\dot{W}^{el}_{LNCMI}$), the heat pump's electricity consumption ($\dot{W}^{el}_{HP}$), and the Heat Supplier's exergy input ($\dot{E}^{in}_{HS}$).

$$\varepsilon_{GLOB} = 1 - \frac{E^{D}_{GLOB}}{E^{in}_{GLOB}} \tag{10}$$

$$\text{With } E^{D}_{GLOB} = \sum_{t=t_{ini}}^{t=t_f} \left(\dot{E}^{D}_{LNCMI} + \dot{E}^{D}_{DISS} + \dot{E}^{L}_{TES} + \dot{E}^{D}_{HP} + \dot{E}^{D}_{HS} + \dot{E}^{D}_{DHN} + \dot{E}^{D}_{SST} \right) \cdot \Delta t \tag{11}$$

$$E^{in}_{GLOB} = \sum_{t=t_{ini}}^{t=t_f} \left[\dot{W}^{el}_{LNCMI} + \dot{W}^{el}_{HP} + \dot{E}^{in}_{HS} \right] \cdot \Delta t \tag{12}$$

The Net Present Value of the project (*NPV*) was the main economic indicator (eq. 13). It is the difference between the revenues from selling heat to the residential end-users ($\dot{C}^{P}_{WHRS}$) and the breakeven revenues ($\dot{C}^{P,BEP}_{WHRS}$). The BreakEven Point (BEP) is the point at which the sales revenues equal the total costs of production. In this study, the breakeven revenues (eq. 14) have to compensate the cost of waste heat ($\dot{C}^{q,out}_{LNCMI}$), the cost of electricity to run the heat pump ($\dot{C}^{elec,in}_{HP}$), and the amortization costs for the heat pump ($\dot{Z}_{HP}$) and the storage ($\dot{Z}_{TES}$). Fuel savings by the district's Heat Supplier ($\dot{C}^{F}_{HS,REF} - \dot{C}^{F}_{HS}$) were considered as a collateral profit, because a Consortium is assumed between all stakeholders involved in the heat valorization process.

$$NPV = \frac{\dot{C}^{P}_{WHRS} - \dot{C}^{P,BEP}_{WHRS}}{CRF} \tag{13}$$

$$\text{With } \dot{C}^{P,BEP}_{WHRS} = \dot{C}^{q,out}_{LNCMI} + \dot{C}^{elec,in}_{HP} + \dot{Z}_{HP} + \dot{Z}_{TES} - \left(\dot{C}^{F}_{HS,REF} - \dot{C}^{F}_{HS} \right) \tag{14}$$

If the sales revenues exceed the breakeven revenues, the project yields net benefits (*NPV* > 0). If both are equal, the investments (including interest) and the production costs are recovered (*NPV* = 0). If the actual revenues are below the breakeven revenues, the *NPV* becomes negative and the project yields net economic losses.

An additional economic indicator was defined for a more detailed analysis: the relative Revenue Requirement of each unit (RR). It indicates which amount of the product's final cost ($\dot{C}^{P}_{WHRS}$) amortizes expenditures on which unit (eq. 15). Those expenditures are capital investments ($\dot{Z}$) plus exogenous consumption of fuel ($\dot{C}^{F,exo}$), i.e. external to the overall district's boundaries. The total revenue requirement for a system is the revenue that must be collected through the sale of all products to compensate for all expenditures incurred and to ensure sound economic operation [11].

$$RR = \left(\dot{Z} + \sum \dot{C}^{F,exo} \right) / \dot{C}^{P}_{WHRS} \tag{15}$$

The overall costs of the irreversibilities ($\dot{C}^{D}_{GLOB}$) were chosen as exergoeconomic indicator (eq. 16). They are the sum of exergy destruction costs of all units ($\dot{C}^{D}$, eq. 17). Note how these costs do not appear explicitly in the cost flow balance (eq. 3). They are usually referred to as *hidden costs* [11].

$$\dot{C}^{D}_{GLOB} = \sum \dot{C}^{D} \tag{16}$$

$$\text{With } \dot{C}^{D} = c^{F} \dot{E}^{D} \tag{17}$$

2.6. Preliminary assessment of multi-criteria optimality

The preliminary multi-criteria Pareto-optimal solution was determined by quantifying and comparing the relative performances of all possible solutions. The relative mono-criteria performance of each solution assessed its proximity to the optimal value of the indicator amongst all available solutions. The equation applied was either 18 when the indicator's value had to be maximized, or 19 when it had to be minimized. The relative multi-criteria performance was assessed through an equally-weighted average of all relative mono-criteria performances (eq. 20).

$$\psi_j^{mono}(maximize) = 1 - \frac{\chi^{max} - \chi_j}{\chi^{max} - \chi^{min}} \tag{18}$$

$$\psi_j^{mono}(minimize) = 1 - \frac{\chi_j - \chi^{min}}{\chi^{max} - \chi^{min}} \tag{19}$$

$$\psi^{multi} = \sum_j \left(w_j \cdot \psi_j^{mono}\right) \quad \left\{\sum_j w_j = 1\right\} \tag{20}$$

3. Results and discussion

3.1. Mono-criterion analyses and optimal conceptions

This study aims to identify the most promising design of a waste heat recovery system through multi-criteria analysis. The four criteria considered are energy, exergy, economy and exergo-economy. The two design parameters under analysis are inlet temperature and thermal storage capacity. There are three inlet temperatures to choose from: 35 °C, 50 °C and 85 °C. There are five storage capacities to choose from: 0 MWh, 10 MWh, 20 MWh, 30 MWh and 40 MWh.

Figure 3 shows the evolution of the energetic and economic indicators (*RACF* and *NPV*, respectively) as a function of the storage capacity and the waste heat's temperature. The color transition along the green arrows (from light to dark) indicates the objective of the optimization, i.e. either to maximize or to minimize. Thus, in Fig. 3 the objectives are to maximize both indicators. The energetic indicator recommends the highest possible temperature (85 °C) and storage capacity (40 MWh). On the other hand, the economic indicator suggests 50 °C and points out that there is no further profit beyond the optimal capacity of 20 MWh.

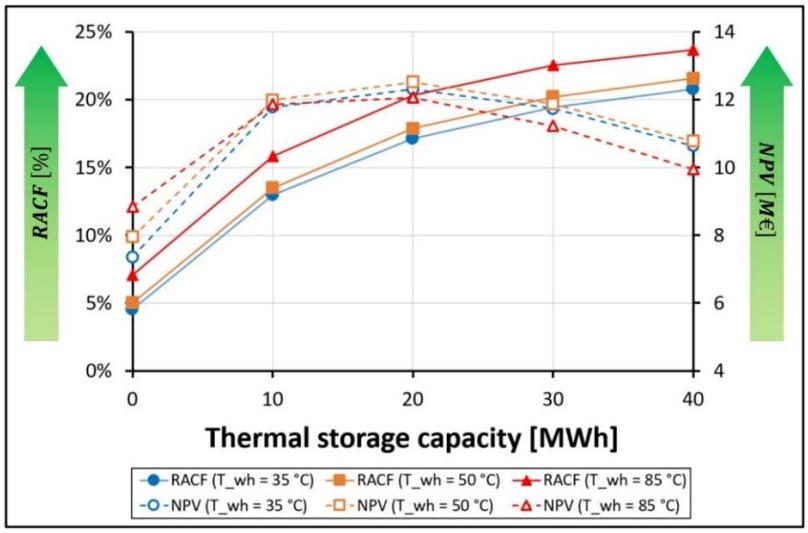

Figure 3. Recovery And Coverage Factor (*RACF*) and Net Present Value (*NPV*) as a function of thermal storage capacity, for the three input temperatures.

Any scenario with heat recovery is better than the base scenario, both energy-wise and economy-wise. Additional heat recovery is asymptotic with respect to additional storage capacity, because of temporal mismatch between the source and the district network. The asymptote is slightly visible on the *RACF*'s evolution. Meanwhile, marginal investment costs increase linearly with additional storage capacity. Beyond 20 MWh, the marginal profit does not outweigh marginal investment costs, at any temperature. This energy/economy divergence confirms the need for a compromise that was already forecasted in the conclusions of the author's previous study.

From the energy standpoint, 85 °C is better because the recovery system takes in more waste heat than the heat pump, and can inject to the district network the same thermal power or even more, because it is not limited by the heat pump's maximal power output. From an economic standpoint, the scenarios at 50 ˚C are the best for the majority of storage capacities. They are better than those at 35 ˚C because the heat pump consumes less electricity, the most expensive 'fuel' in this case study. As an added benefit it takes in more waste heat, thus the *RACF* is higher. At 85 °C, only the case without storage is more profitable than the other temperatures. The reason for this is that no investment on a heat pump is necessary. But at 10 MWh and beyond, the costs of waste heat outweigh the profits. This happens because LNCMI's waste heat has a much higher price at 85 °C than at 35 °C or 50 °C, due to the decreased electricity-to-heat conversion ratio (refer to Table 1).

Figure 4 presents the evolution of the exergetic and exergoeconomic indicators (E^D_{GLOB} and C^D_{GLOB}, respectively). Unlike the energy/economy pair, these indicators recommend 35 ˚C as input temperature. Waste heat at higher temperatures is not optimal exergy-wise because of the increased electric consumption of the LNCMI's magnets and the increased losses. The same reasoning applies in exergo-economics, aggravated by higher costs of LNCMI's waste heat at higher temperatures. This increases other specific costs downstream in the district. In the reference case, the overall exergy destruction is 20.6 GWh/year and the overall exergy destruction cost is 3.09 M€/year. By comparing those data with the points in Fig. 4, it can be seen that all designs except those at 85 °C are better. Refer to the tables in Appendix B for detailed results of the reference and optimal scenarios.

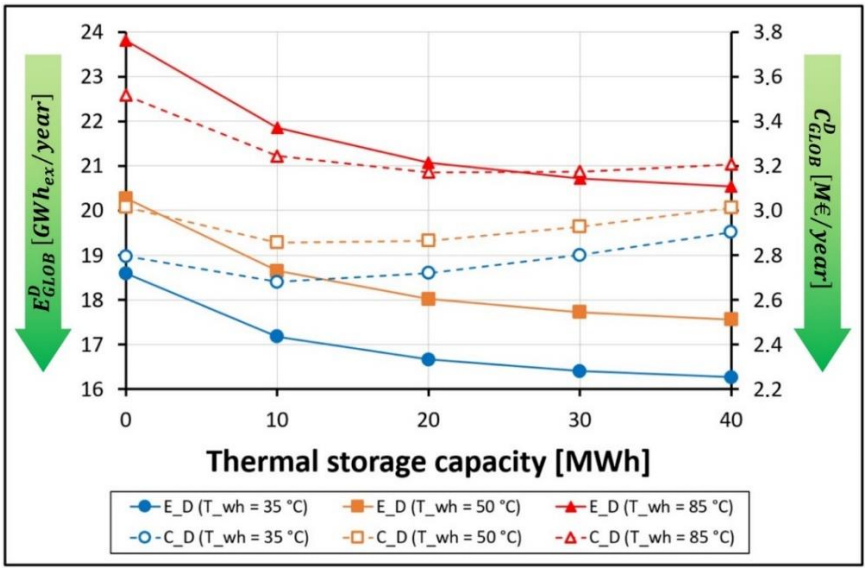

Figure 4. Overall annual irreversibilities (E^D_{GLOB}) and annual cost of irreversibilities (C^D_{GLOB}) as a function of thermal storage capacity, for the three input heat temperatures.

As for the storage capacity, a discrepancy similar to that observed in Fig. 3 is observed here. The exergetic indicator suggests the largest possible storage (40 MWh), while exergo-economy finds its optimum at 10 MWh. Beyond 10 MWh, the benefits of recovering more waste heat are outweighed by the marginal investment costs. At T_{wh} = 85 ˚C,

the turning point exists at 20 MWh instead. The explanation for this is the absence of a heat pump and its associated exergy destruction costs.

Table 2 shows the values of the performance indicators for each monocriterion-optimal scenario. For the sake of comparison, the exergetic and exergoeconomic metrics of the recovery system alone are also shown. It is worth mentioning that if the assessment was applied only on the recovery system, the selected design would be different: The exergy-focused optimization would prefer T_{wh} = 85 ˚C with U_{TES}^{max} = 40 MWh instead of T_{wh} = 35 ˚C with U_{TES}^{max} = 40 MWh. Furthermore, an optimization focused on exergoeconomics would prefer T_{wh} = 85 ˚C with U_{TES}^{max} = 40 MWh instead of T_{wh} = 35 ˚C with U_{TES}^{max} = 10 MWh. This reflects the importance of the systemic approach considering all units affected by the heat recovery, even those that do not belong to the industrial process itself.

Table 2. Values of the performance indicators for each mono-criterion optimal design.

Design	$RACF$ (%)	NPV ($M€$)	E_{GLOB}^{D} ($GWh_{ex}/year$)	C_{GLOB}^{D} ($M€/year$)	$[E_{WHRS}^{D}]$ ($GWh_{ex}/year$)	$[C_{WHRS}^{D}]$ ($k€/year$)
ENER-optimal {T_{wh} = 85 °C, U_{TES}^{max} = 40 MWh}	23.7	9.95	20.55	3.21	0.006	1.23
ECON-optimal {T_{wh} = 50 °C, U_{TES}^{max} = 20 MWh}	17.9	12.5	18.02	2.87	1.180	266
EXER-optimal {T_{wh} = 35 °C, U_{TES}^{max} = 40 MWh}	20.8	10.6	16.27	2.90	2.047	525
EXEC-optimal {T_{wh} = 35 °C, U_{TES}^{max} = 10 MWh}	13.0	11.8	17.18	2.28	1.618	272

Figure 5 presents a detailed trace of the overall process from the exergetic, exergoeconomic and economic points of view. All these indicators are represented per MWh of heat delivered to the residential end-users, and the optimization objective was to minimize their values.

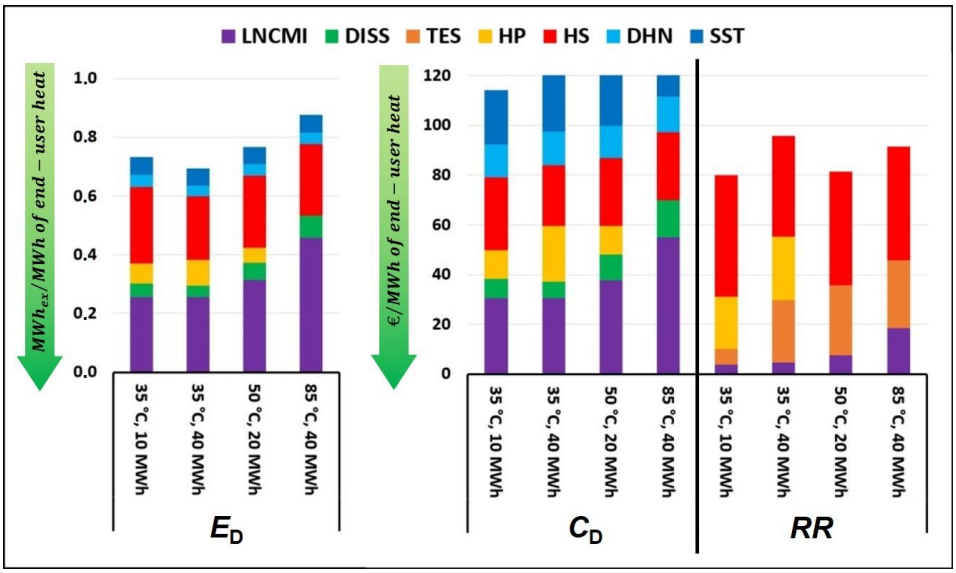

Figure 5. Detailed "4E pathway" of the overall system. All indicators are expressed per MWh of heat delivered to the residential end-users.

This can be considered a "4E pathway" of the overall system, as if all units in the district were part of a same process meant to deliver heat to end-users. From waste heat rejection at the LNCMI up to the residential clients, each unit increases irreversibility, the cost of irreversibility, and in most cases the product's final cost. The bar charts in the

figure allow to identify each contribution. Although no energetic indicator is presented, energy is implicit in all other criteria, since the four models are internally correlated. It is also important to bear in mind that the C_{GLOB}^{D} and the sum of all RR_k must not be directly contrasted in this figure. The first one refers to the overall scenario and includes irreversibilities that do not need to be amortized by the heat sold to residential end-users. Likewise, exergy destruction is accounted for all units in the scenario, not only those involved in the injection of heat to the district network. That explains its relatively high values.

The "4E pathway" contains useful information. For instance, almost half of the contributions to the irreversibilities and their costs are related to the LNCMI's activities. Moreover, note how LNCMI's influence on those indicators increases at higher temperatures. The effect of waste heat temperature at 85 °C is slightly noticeable at the dissipation unit, too. Another effect is that the influence of the HP is not there anymore. This is especially noticeable in the revenue requirement, since the heat pump represents a high investment whenever it is included. The effect of increasing the storage capacity is quite noticeable on the revenue requirement, too: the *RR* related to the storage increases by 4-fold. Meanwhile, the thermal storage unit has barely any influence on the other two indicators. Note also that the dissipation unit, the district heating and the substations do not have any influence on the *RR*, because they use no external paid-for fuel nor require any additional investment.

The *RR* also gives an idea of how profitable the project can be. As mentioned in the hypotheses, the final price of heat for the consumers is set at 80 €/MWh. If the aggregated *RR* is below that mark, the difference means benefits. The larger the difference, the more the profit. Note that with some of the designs, the heat's revenue requirement exceeds 80 €/MWh. Thus, that design has a positive *NPV* (Fig. 3) only thanks to the Heat Supplier's indirect benefit due to less fuel consumption. As mentioned in the hypotheses, that benefit was mutualized between all of the project's stakeholders, respecting a Consortium.

A general conclusion from Fig. 5 is that a component does not necessarily have the same influence on every criterion. For example, at 35 °C note how the LNCMI's process has the considerable weights of around 40 % and 30 % in the exergy and exergo-economic criteria, respectively, but only of 5-20 % in the revenue requirement. This is because the electro-intensive process has important irreversibilities, but its waste heat is sold at relatively low prices. As another example, note how the heat supplier's influence is prominent on the revenue requirement (between 40 % and 50 %), but smaller on the costs of irreversibilities (around 20%). This may be explained because their fuel is relatively expensive, but their process is rather exergy-efficient. For the sake of information, Appendix B shows detailed metrics unit by unit for all mono- and multi-criteria optimal scenarios.

3.2. Dual-criteria Pareto-optimal conceptions

This analysis aims to clarify which compromises can be achieved between mono-criterion optimal conceptions. As a reminder, the following non-redundant optimal solutions have been identified in the previous section:

- $T_{wh} = 85\ °C$ and $U_{TES}^{max} = 40\ MWh$ is the energetically (ENER) optimal design.
- $T_{wh} = 35\ °C$ and $U_{TES}^{max} = 40\ MWh$ is the exergetically (EXER) optimal design.
- $T_{wh} = 50\ °C$ and $U_{TES}^{max} = 20\ MWh$ is the economically (ECON) optimal design.
- $T_{wh} = 35\ °C$ and $U_{TES}^{max} = 10\ MWh$ is the exergo-economically (EXEC) optimal design.

These results have two main consequences for the multi-criteria analyses. First, none of the criteria are redundant. Second, there exist two types of Pareto fronts: as a function of T_{wh} and as a function of U_{TES}^{max}. Although both types are scientifically interesting, only those related to U_{TES}^{max} were studied here. The fronts related to T_{wh} are somewhat

discouraging to analyze for this case, because: 1) The gap between $T_{wh} = 50\,°C$ and $T_{wh} = 85\,°C$ does not find practical application due to technological constraints of the magnets' cooling loop; 2) The case at $T_{wh} = 85\,°C$ has important technological differences, and belongs therefore to a different Pareto front of which only 1 point ($T_{wh} = 85\,°C$) finds practical application.

The 4 non-redundant criteria can lead to up to 6 dual-criteria Pareto fronts. Those are presented in the following figures. Like in the previous figures, arrows with color transition from light green to dark green indicate the optimization objectives. Figure 6 introduces the energy-economy and exergoeconomics-economy relationships.

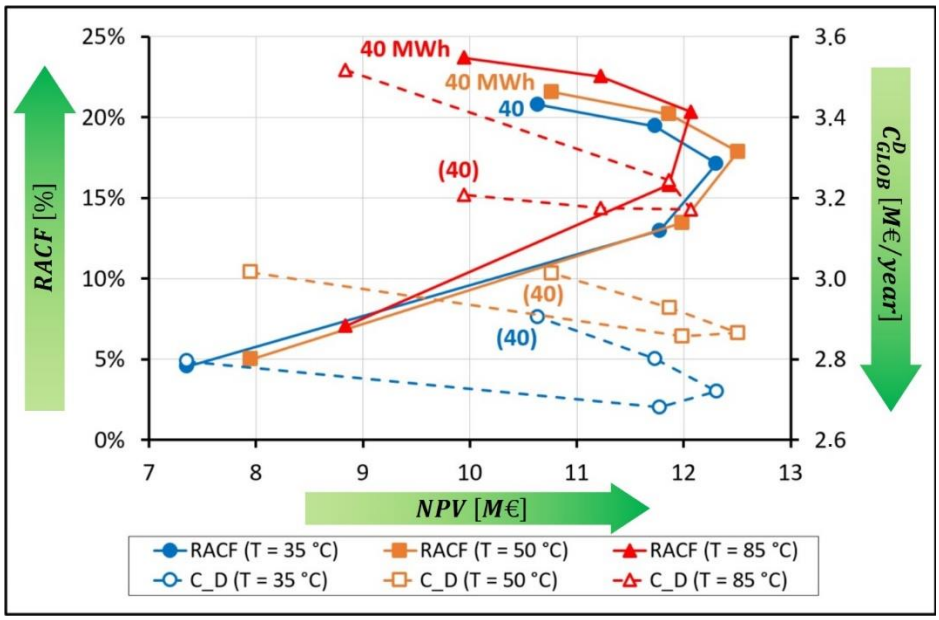

Figure 6. Energy-economy Pareto front (*RACF* vs *NPV*) and exergoeconomics-economy Pareto front (C^D_{GLOB} vs *NPV*) as a function of thermal storage capacity, for the three input heat temperatures.

The energy-economy Pareto-optimal frontier is made up by the designs at 85 ˚C between 20 MWh and 40 MWh, plus the design at 50 °C with 20 MWh. These four solutions dominate all other solutions. Increasing thermal storage capacity has consistent energetic benefits at the expense of profitability. Switching from 50 °C - 20 MWh to 85 °C - 20 MWh increases the *RACF* from 17.9% to 20.3% in exchange for only 3.6% less profit. Then, keeping *T* = 85 °C while increasing storage capacity from 20 MWh to 30 MWh increases the *RACF* further to 22.5%, but in exchange for a further drop of 7% in profitability already. In the final increase from 30 MWh to 40 MWh, the margins look discouraging: a further drop of 11% in profits, for only a slight increase in the *RACF* to 23.7%.

The exergoeconomics-economy analysis presents as most promising the following solutions: {50 °C - 20 MWh}, {35 °C - 10 MWh} and {35 °C - 20 MWh}. The economic indicator prioritizes the solution at {50 °C - 20 MWh}, while the exergoeconomic indicator prioritizes the {35 °C – 10 MWh} solution. The {35 °C – 20 MWh} solution seems like a healthy compromise between the two. None of the solutions at 85 °C is promising in the exergoeconomics-economy analysis. Besides, at 85 °C the evolution of the exergoeconomic indicator is opposite with respect to the other temperatures because of the absence of heat pump, and because the turning point is different (Fig. 4).

Figure 7 presents the energy-exergy and economy-exergy analyses. In the first one, there is actually no storage-dependent Pareto front. Greater storage capacities lead to a better *RACF* and less irreversibility, straightforwardly. However, their marginal improvement slows down at each increase in capacity. Depending on the unfavorable evolution of other indicators, it may be sensible to not pursue the largest storage unit. This has been observed in the

energy-economy comparison from Fig. 6, for instance. The design temperature of 50 °C is surpassed exergy-wise by T = 35 ˚C and energy-wise by T = 85 ˚C, but it might yield good compromises between those two temperatures.

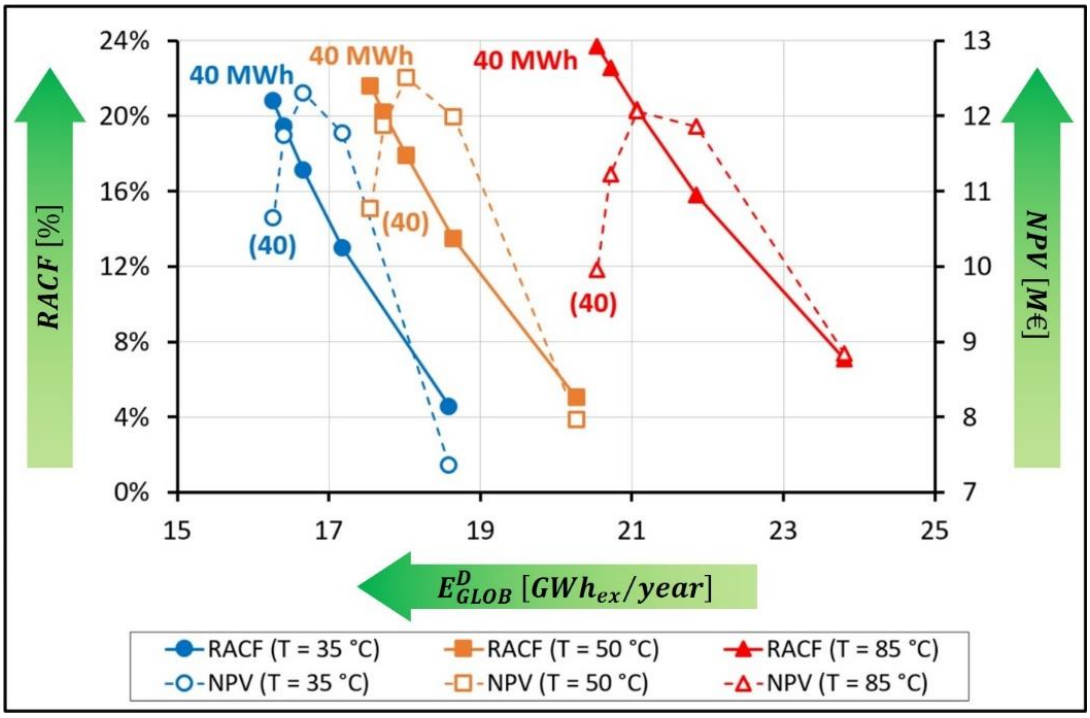

Figure 7. Energy-exergy Pareto front (*RACF* vs E^D_{GLOB}) and economy-exergy Pareto front (*NPV* vs E^D_{GLOB}) as a function of thermal storage capacity, for the three industrial waste heat temperatures.

The economy-exergy analysis, on the contrary, has tendencies that are less intuitive. The {35 °C - 40 MWh}, {35 °C - 30 MWh} and {35 °C - 20 MWh} solutions outperform any other solution exergy-wise. Meanwhile, the {50 °C - 20 MWh} solution outperforms any other solution economy-wise. Switching successively from {35 °C - 40 MWh} to the next designs in the Pareto frontier yields marginal increases in net profit at the expense of exergy efficiency. The inlet temperature of 85 °C is dominated by the other temperatures in the economy-exergy analysis. With respect to Fig. 6, this figure adds 2 new candidates to the list of promising designs.

The results found for 20 MWh reinforce a perspective mentioned in the Conclusions of the authors' previous article. In theory, it is feasible for the LNCMI to adjust dynamically the temperature of their waste heat, as a function of temporal mismatch between their activities and the district's thermal needs. A storage capacity of 20 MWh may fit well in such strategy, because the recovery system would always operate on its economy-exergy Pareto front at either 35 °C or 50 °C. The same consideration applies on the economy-exergoeconomics Pareto frontier shown in Fig. 6. For extensive results, Figure B.1 in Appendix B contains additional Pareto fronts.

Table 3 summarizes the main conclusions from analyzing the Pareto fronts generated through analyses based on energy (ENER), exergy (EXER), economy (ECON) and exergoeconomics (EXEC). Solutions displayed in bold font are monocriterion-optimal, while the rest are Pareto-optimal. Among the Pareto-optimal solutions, those which prioritize one of the criteria are indicated with the suffix "Promising". If a Pareto-optimal solution is nearly halfway between the two optimal values, it is labeled as a "Compromise". The cells with no information in them mean that the design is not interesting with respect to that front. The energy-exergy analysis is not included in the table because it has no Pareto front and optimality is straightforward.

Table 3. Performance of each possible design with respect to each dual-criteria Pareto front.

Solution \ Front	ENER-ECON	ENER-EXEC	ECON-EXER	ECON-EXEC	EXER-EXEC
{35 °C, 0 MWh}	-	-	-	-	-
{35 °C, 10 MWh}	-	**EXEC-Optimal**	-	**EXEC-Optimal**	**EXEC-Optimal**
{35 °C, 20 MWh}	-	EXEC-Promising	ECON-Promising	Compromise	EXEC-Promising
{35 °C, 30 MWh}	-	EXEC-Promising	EXER-Promising	-	EXER-Promising
{35 °C, 40 MWh}	-	Compromise	**EXER-Optimal**	-	**EXER-Optimal**
{50 °C, 0 MWh}	-	-	-	-	-
{50 °C, 10 MWh}	-	-	-	-	-
{50 °C, 20 MWh}	**ECON-Optimal**	-	**ECON-Optimal**	**ECON-Optimal**	-
{50 °C, 30 MWh}	-	-	-	-	-
{50 °C, 40 MWh}	-	Compromise	-	-	-
{85 °C, 0 MWh}	-	-	-	-	-
{85 °C, 10 MWh}	-	-	-	-	-
{85 °C, 20 MWh}	ECON-Promising	-	ECON-Promising	ECON-Promising	-
{85 °C, 30 MWh}	ENER-Promising	ENER-Promising	-	-	-
{85 °C, 40 MWh}	**ENER-Optimal**	**ENER-Optimal**	-	-	-

The semi-qualitative analysis allowed to discard a few solutions that are not promising from any point of view. On the other hand, those that are optimal or Pareto-optimal in at least one front have a chance of becoming multi-criteria optimal. Especially, the {35 °C – 20 MWh} and {35 °C – 30 MWh} solutions have some fair chances. Despite not being optimal in any criterion, they are Pareto-optimal in at least 3 out of 5 different fronts. Thus, they seem the strongest candidates for multicriteria optimality. Of course, the concept of 'optimality' depends on criteria weights.

In addition to information on the designs, this analysis has given information about the fronts, too. Namely, the exergy-exergoeconomics front is the most restrictive one in terms of temperature, since it only accepts 35 °C as promising. That can make this front hard to conciliate with others. In terms of storage capacity, the economy-exergoeconomics front is clearly the most restrictive, since it restricts promising solutions to a storage capacity of either 10 MWh or 20 MWh. The rest of the fronts are quite flexible in temperature or in storage capacity, with the energy-exergoeconomics front being the most flexible.

Next section shows results for the quantitative multicriteria analysis. Those results may or may not confirm the {35 °C – 20 MWh} and {35 °C – 30 MWh} solutions as the most promising ones, as pointed out by the semi-qualitative analysis.

3.3. Preliminary results about multi-criteria optimality

Table 4 shows multi-criteria optimality for each scenario, assuming that all criteria are equally important to the decision-maker. The table confirms quantitatively what was perceived semi-qualitatively in the dual-criteria analysis. The {35 ˚C – 30 MWh} design shows high performance in almost every criterion, and that sets it apart as optimal solution. The {35 ˚C – 20 MWh} design is almost as suitable, but more inclined towards economy and exergoeconomics. Remarkably, none of the two were in the list of mono-criteria optimal designs. It is also remarkable that the 3 highest multi-criteria performances involve waste heat at 35 ˚C. This means that the multicriteria optimum in this case study is strongly influenced by exergy and exergoeconomics. In terms of thermal storage capacity, the multicriteria optimum is a compromise between economic and non-economic criteria.

Table 4. Proximity of each scenario to multi-criterion optimality.

Design	Mono/Dual-criteria optimality	ψ_{ENER}^{mono} (*w* = 0.25)	ψ_{EXER}^{mono} (*w* = 0.25)	ψ_{ECON}^{mono} (*w* = 0.25)	ψ_{EXEC}^{mono} (*w* = 0.25)	ψ^{multi}
35 °C. REF	None	0%	62%	0%	73%	33.7%
35 °C. 0 MWh	None	19%	80%	59%	92%	62.5%
35 °C. 10 MWh	EXEC-Optimal	55%	92%	94%	**100%**	85.2%
35 °C. 20 MWh	**Multicriteria-Suboptimal**	72%	97%	98%	97%	**91.2%**
35 °C. 30 MWh	**Multicriteria-Optimal**	82%	99%	94%	92%	**91.7%**
35 °C. 40 MWh	EXER-Optimal	88%	**100%**	85%	85%	89.5%
50 °C. REF	None	0%	43%	0%	51%	23.6%
50 °C. 0 MWh	None	21%	65%	64%	78%	56.9%
50 °C. 10 MWh	None	57%	79%	96%	88%	80.1%
50 °C. 20 MWh	ECON-Optimal	75%	85%	**100%**	88%	87.0%
50 °C. 30 MWh	None	85%	87%	95%	83%	87.7%
50 °C. 40 MWh	ENER/EXEC-Compromise	91%	89%	86%	78%	85.9%
85 °C. REF	None	0%	0%	0%	0%	0.0%
85 °C. 0 MWh	None	30%	34%	71%	44%	44.7%
85 °C. 10 MWh	None	67%	51%	95%	62%	68.8%
85 °C. 20 MWh	ECON-Promising	86%	58%	96%	67%	76.9%
85 °C. 30 MWh	ENER-Promising	95%	61%	90%	67%	78.3%
85 °C. 40 MWh	ENER-Optimal	**100%**	63%	80%	65%	76.8%

If each criterion had a different weight, it might be easier to decide between {35 ˚C – 20 MWh} or {35 ˚C – 30 MWh}. But in this case all of them have the same importance, so the final decision would be in the investors' hands. This result serves as a reminder that multi-criteria analyses are just support tools, and final decisions belong to human choices. Of course, there exist more robust (and complex) methods for multi-criteria decision making, such as the ELECTRE family of methods [49].

4. Conclusions and perspectives

This study has determined the most promising inlet temperature and thermal storage capacity of an industrial waste heat recovery system for district heating, by means of a systemic-anticipative approach with 4E analyses (energy, exergy, economy and exergoeconomics) based on local balances. These 4E analyses have been applied on an operating scenario where the management of energy flows had been previously optimized on an hourly time step for a whole year, using Mixed-Integer Linear Programming. The main conclusions of this study are:

- The most promising design is an inlet temperature of 35 °C and a storage capacity of 30 MWh.
- With that design, the system recovers 41% of the total waste heat, covers 48% of the total residential heat demands, and has an estimated Net Present Value of 11.7 M€ over 20 years. In comparison to the base scenario, the heat recovery system reduces the district's overall exergy destruction and exergy destruction costs by 20% (4.2 GWh/year) and 9% (286 k€/year), respectively.

- None of the mono-criterion assessments pointed out this design as optimal. Therefore, the multicriteria systemic assessment was of utmost importance to detect the most promising solution.
- Fundamental discrepancies between indicators have been identified. Exergy and exergoeconomics recommend the lowest possible temperature (35 °C), while energy-based indicators tend to recommend the highest possible temperature (85 °C). Meanwhile, the economic indicator recommended 50 °C in this case study. This reinforces the interest of including exergy-based indicators in the analyses, since they suggest non-redundant solutions. In addition, technical indicators recommend the largest possible storage capacity (40 MWh) while economy-related indicators advise to stay around 10-20 MWh.

- The most promising design implies a temperature of 35 °C. Therefore, the exergy-related indicators had a strong presence in the final solution, despite being assigned the same weight as other criteria. This reinforces the interest of exergy and exergoeconomics as criteria for decision-making in waste heat recovery, district heating and urban planning.

Two main perspectives have been identified after this study. The first one is to explore two advanced strategies for better heat valorization: 1) Re-schedule the LNCMI laboratory's yearly calendar of experiments, to synchronize them with the periods of highest residential heat demands; 2) Adjust the magnets' cooling loop to reject heat at higher temperatures when there are residential demands, and at lower temperatures the rest of the time. The storage capacity of 20 MWh seems a good candidate for the second strategy, because the system can operate at Pareto-optimality at any of the three temperatures.

The second perspective is to use a multi-actor approach to model more realistic scenarios. Indeed, this article assumed a consortium between all potential investors, but in reality the recovery system may belong solely to the industrial actor, the district network operator, or even a third stakeholder. Depending on ownership of the heat recovery system, the most suitable design can change significantly.

Acknowledgement

The authors are grateful to La Région Auvergne-Rhône-Alpes for their financial support through the OREBE projet (Optimisation holistique des Réseaux d'Energie et des Bâtiments producteurs d'énergies dans les Eco-quartiers). They are also grateful to the ADEME (the French Agency for Environment and Energy Management) for their financial support through the RETHINE project (Réseaux Electriques et THermiques InterconNEctés). This work has been partially supported by the CDP Eco-SESA receiving fund from the French National Research Agency in the framework of the "Investissements d'avenir" program (ANR-15-IDEX-02).

The authors thank the other members of the developer team of the optimization tool used in this study, OMEGAlpes, especially Lou Morriet (G2Elab and PACTE, Grenoble) and Benoit Delinchant (G2Elab, Grenoble).

The authors thank the corresponding decision-makers from the French National Laboratory of High-intensity Magnetic Fields (LNCMI) for: Facilitating real operational data to construct the model hourly energy profile of electricity consumption used in this study; Allowing to publish that hourly profile in the articles; And for allowing to make the data available in the OMEGAlpes Documentation [44] for public use under license (ODC-By v1.0).

References

[1] Rezaie B, Rosen MA. District heating and cooling : Review of technology and potential enhancements. Appl Energy 2012;93:2–10. doi:10.1016/j.apenergy.2011.04.020.

[2] Schmidt D, Kallert A, Blesl M, Li H, Svendsen S, Nord N. IEA Annex TS1: Low Temperature District Heating for Future Energy

Systems - Final report - Future low temperature district heating design guidebook. AGFW-Project Company, Frankfurt Am Main (Germany): 2017.

[3] Jouhara H, Olabi AG. Editorial: Industrial waste heat recovery. Energy 2018;160:1–2. doi:10.1016/j.energy.2018.07.013.

[4] McKenna RC, Norman JB. Spatial modelling of industrial heat loads and recovery potentials in the UK. Energy Policy 2010;38:5878–91. doi:10.1016/j.enpol.2010.05.042.

[5] Svensson IL, Jönsson J, Berntsson T, Moshfegh B. Excess heat from kraft pulp mills: Trade-offs between internal and external use in the case of Sweden-Part 1: Methodology. Energy Policy 2008;36:4178–85. doi:10.1016/j.enpol.2008.07.017.

[6] Jönsson J, Svensson IL, Berntsson T, Moshfegh B. Excess heat from kraft pulp mills: Trade-offs between internal and external use in the case of Sweden-Part 2: Results for future energy market scenarios. Energy Policy 2008;36:4186–97. doi:10.1016/j.enpol.2008.07.027.

[7] Miró L, Brueckner S, McKenna R, Cabeza LF. Methodologies to estimate industrial waste heat potential by transferring key figures: A case study for Spain. Appl Energy 2016;169:866–73. doi:10.1016/j.apenergy.2016.02.089.

[8] ADEME. La chaleur fatale. Technical report. Angers (France): 2017.

[9] Lund H, Werner S, Wiltshire R, Svendsen S, Thorsen JE, Hvelplund F, Vad Mathiesen B. 4th Generation District Heating (4GDH) - Integrating smart thermal grids into future sustainable energy systems. Energy 2014;68:1–11. doi:10.1016/j.energy.2014.02.089.

[10] Sangi R, Müller D. A novel hybrid agent-based model predictive control for advanced building energy systems. Energy Convers Manag 2018;178:415–27. doi:10.1016/j.enconman.2018.08.111.

[11] Bejan A, Tsatsaronis G, Moran M. Thermal Design and Optimization. 1st ed. Canada: John Wiley & Sons; 1996.

[12] Fitó J, Hodencq S, Ramousse J, Wurtz F, Stutz B, Debray F, Vincent B. Energy- and exergy-based optimal designs of a low-temperature industrial waste heat recovery system in district heating. Energy Convers Manag 2020;211:Article number 112753. doi:10.1016/j.enconman.2020.112753.

[13] Tsatsaronis G. Definitions and nomenclature in exergy analysis and exergoeconomics. Energy 2007;32:249–53. doi:10.1016/j.energy.2006.07.002.

[14] Lazzaretto A, Tsatsaronis G. SPECO: A systematic and general methodology for calculating efficiencies and costs in thermal systems. Energy 2006;31:1257–89. doi:10.1016/j.energy.2005.03.011.

[15] Lior N, Zhang N. Energy , exergy , and Second Law performance criteria 2007;32:281–96. doi:10.1016/j.energy.2006.01.019.

[16] Dincer I. The role of exergy in energy policy making. Energy Policy 2002;30:137–49. doi:10.1016/S0301-4215(01)00079-9.

[17] Bühler F, Nguyen T Van, Elmegaard B. Energy and exergy analyses of the Danish industry sector. Appl Energy 2016;184:1447–59. doi:10.1016/j.apenergy.2016.02.072.

[18] Solheimslid T, Harneshaug HK, Lümmen N. Calculation of first-law and second-law-efficiency of a Norwegian combined heat and power facility driven by municipal waste incineration-A case study. Energy Convers Manag 2015;95:149–59. doi:10.1016/j.enconman.2015.02.026.

[19] Wang J, Wang Z, Zhou D, Sun K. Key issues and novel optimization approaches of industrial waste heat recovery in district heating systems. Energy 2019;188:116005. doi:10.1016/j.energy.2019.116005.

[20] Baldvinsson I, Nakata T. A comparative exergy and exergoeconomic analysis of a residential heat supply system paradigm of Japan and local source based district heating system using SPECO (specific exergy cost) method. Energy 2014;74:537–54. doi:10.1016/j.energy.2014.07.019.

[21] Zhang J, Ge B, Xu H. An equivalent marginal cost-pricing model for the district heating market. Energy Policy 2013;63:1224–32. doi:10.1016/j.enpol.2013.09.017.

[22] Čož TD, Kitanovski A, Poredoš A. Exergoeconomic optimization of a district cooling network. Energy 2017;135:342–51. doi:10.1016/j.energy.2017.06.126.

[23] Hepbasli A. A review on energetic, exergetic and exergoeconomic aspects of geothermal district heating systems (GDHSs). Energy Convers Manag 2010;51:2041–61. doi:10.1016/j.enconman.2010.02.038.

[24] Keçebaş P, Gökgedik H, Alkan MA, Keçebaş A. An economic comparison and evaluation of two geothermal district heating systems for advanced exergoeconomic analysis. Energy Convers Manag 2014;84:471–80. doi:10.1016/j.enconman.2014.04.068.

[25] Sanaye S, Amani M, Amani P. 4E modeling and multi-criteria optimization of CCHPW gas turbine plant with inlet air cooling and steam injection. Sustain Energy Technol Assessments 2018;29:70–81. doi:10.1016/j.seta.2018.06.003.

[26] Akrami E, Ameri M, Rocco M V., Sanvito FD, Colombo E. Thermodynamic and exergo-economic analyses of an innovative semi self-feeding energy system synchronized with waste-to-energy technology. Sustain Energy Technol Assessments 2020;40:100759. doi:10.1016/j.seta.2020.100759.

[27] Shahnazari A, Rafiee M, Rohani A, Bhushan Nagar B, Ebrahiminik MA, Aghkhani MH. Identification of effective factors to select energy recovery technologies from municipal solid waste using multi-criteria decision making (MCDM): A review of thermochemical technologies. Sustain Energy Technol Assessments 2020;40. doi:10.1016/j.seta.2020.100737.

[28] Liu X, Yang X, Yu M, Zhang W, Wang Y, Cui P, Zhu Z, Ma Y, Gao J. Energy, exergy, economic and environmental (4E) analysis of an integrated process combining CO2 capture and storage, an organic Rankine cycle and an absorption refrigeration cycle. Energy Convers Manag 2020;210:112738. doi:10.1016/j.enconman.2020.112738.

[29] Ameri M, Mokhtari H, Bahrami M. Energy, exergy, exergoeconomic and environmental (4E) optimization of a large steam power plant: A case study. Iran J Sci Technol - Trans Mech Eng 2016;40:11–20. doi:10.1007/s40997-016-0002-z.

[30] Wang J, Lu Z, Li M, Lior N, Li W. Energy, exergy, exergoeconomic and environmental (4E) analysis of a distributed generation solar-assisted CCHP (combined cooling, heating and power) gas turbine system. Energy 2019;175:1246–58. doi:10.1016/j.energy.2019.03.147.

[31] Elbar ARA, Yousef MS, Hassan H. Energy, exergy, exergoeconomic and enviroeconomic (4E) evaluation of a new integration of solar still with photovoltaic panel. J Clean Prod 2019;233:665–80. doi:10.1016/j.jclepro.2019.06.111.

[32] Wang S, Li G, Yang X, Zhao F, Cui P, Qi J, Zhu Z, Ma Y, Wang Y. Theoretical assessment of ketone ammoximation production using thermodynamic, techno-economic, and life cycle environmental analyses. J Clean Prod 2020;264:121557. doi:10.1016/j.jclepro.2020.121557.

[33] Meng D, Dai Y, Xu Y, Wu Y, Cui P, Zhu Z, Ma Y, Wang Y. Energy, economic and environmental evaluations for the separation of ethyl acetate/ethanol/water mixture via distillation and pervaporation unit. Process Saf Environ Prot 2020;140:14–25.

doi:10.1016/j.psep.2020.04.039.

[34] Ajah AN, Patil AC, Herder PM, Grievink J. Integrated conceptual design of a robust and reliable waste-heat district heating system. Appl Therm Eng 2007;27:1158–64. doi:10.1016/j.applthermaleng.2006.02.039.

[35] Ghafghazi S, Sowlati T, Sokhansanj S, Melin S. A multicriteria approach to evaluate district heating system options. Appl Energy 2010;87:1134–40. doi:10.1016/j.apenergy.2009.06.021.

[36] Dorotić H, Pukšec T, Duić N. Economical, environmental and exergetic multi-objective optimization of district heating systems on hourly level for a whole year. Appl Energy 2019;251:113394. doi:10.1016/j.apenergy.2019.113394.

[37] Dénarié A, Muscherà M, Calderoni M, Motta M. Industrial excess heat recovery in district heating: Data assessment methodology and application to a real case study in Milano, Italy. Energy 2019;166:170–82. doi:10.1016/j.energy.2018.09.153.

[38] Wang H, Duanmu L, Lahdelma R, Li X. Developing a multicriteria decision support framework for CHP based combined district heating systems. Appl Energy 2017;205:345–68. doi:10.1016/j.apenergy.2017.07.016.

[39] Fang H, Xia J, Zhu K, Su Y, Jiang Y. Industrial waste heat utilization for low temperature district heating. Energy Policy 2013;62:236–46. doi:10.1016/j.enpol.2013.06.104.

[40] Woolley E, Luo Y, Simeone A. Industrial waste heat recovery: A systematic approach. Sustain Energy Technol Assessments 2018;29:50–9. doi:10.1016/j.seta.2018.07.001.

[41] Oluleye G, Smith R. A mixed integer linear programming model for integrating thermodynamic cycles for waste heat exploitation in process sites. Appl Energy 2016;178:434–53. doi:10.1016/j.apenergy.2016.06.096.

[42] Miró L, Gasia J, Cabeza LF. Thermal energy storage (TES) for industrial waste heat (IWH) recovery: A review. Appl Energy 2016;179:284–301. doi:10.1016/j.apenergy.2016.06.147.

[43] Guelpa E, Verda V. Thermal energy storage in district heating and cooling systems: A review. Appl Energy 2019;252:113474. doi:10.1016/j.apenergy.2019.113474.

[44] Delinchant B, Hodencq S, Maréchal Y, Morriet L, Pajot C, Reinbold V, Wurtz F. OMEGAlpes documentation. Univ Grenoble Alpes, CNRS, Grenoble INP, G2Elab, CEA, Univ Paris-Sud n.d. https://omegalpes.readthedocs.io/en/latest/.

[45] Hodencq S, Debray F, Trophime C, Vincent B, Stutz B, Delinchant B, Wurtz F, Pajot C, Morriet L, Bentivoglio F, Couturier R, Giraud N, Aromatario V. Thermohydraulics of High Field Magnets : from microns to urban community scale. 24ème Congrès Français de Mécanique, Brest (France): 2019.

[46] Ahmed N, Elfeky KE, Lu L, Wang QW. Thermal and economic evaluation of thermocline combined sensible-latent heat thermal energy storage system for medium temperature applications. Energy Convers Manag 2019;189:14–23. doi:10.1016/j.enconman.2019.03.040.

[47] Morriet L, Pajot C, Delinchant B, Marechal Y, Wurtz F, Debray F, Vincent B. Optimisation multi-acteurs appliquée à la valorisation de chaleur fatale d'un acteur industriel flexible. Conférence Francoph. l'International Build. Perform. Simul. Assoc. (IBPSA)., 2018.

[48] Pons M. On the reference state for exergy when ambient temperature fluctuates. Int J Thermodyn 2009;12:113–21.

[49] Greco S, Figueira J, Ehrgott M. Multiple criteria decision analysis. Catania (Italy): 2016.

Appendix A. Detailed equations of the 4E model

Table A.1 contains the concretized energy balances unit by unit, as well as the auxiliary equations.

Table A.1. Concretized formulation of the energy balance for each unit.

Unit	Energy balance	Auxiliary equations
LNCMI	$\dot{W}_{LNCMI}^{in} \cdot \xi = \dot{Q}_{LNCMI}^{out}$	$\xi = 0.85$
DISS	$\dot{Q}_{LNCMI}^{out} = \dot{Q}_{DISS}^{in} + \dot{Q}_{TES}^{in}$	$\dot{Q}_{TES}^{in,max} \leq U_{TES}^{max} / \Delta t_{TES}^{min,chrg}$
TES	$\Delta U_{TES} = \dot{Q}_{TES}^{in} - \dot{Q}_{TES}^{out} - \dot{Q}_{TES}^{L}$	$\dot{Q}_{TES}^{out,max} \leq U_{TES}^{max} / \Delta t_{TES}^{min,dchg}$
HP	$\dot{Q}_{HP}^{in} + \dot{W}_{HP}^{in} = \dot{Q}_{HP}^{out}$ $\dot{Q}_{HP}^{in} = \dot{Q}_{TES}^{out}$ $COP_{HP} = \dot{Q}_{HP}^{out} / \dot{W}_{HP}^{in,elec}$	$COP_{HP}(T_{HP}^{in} = 35\,°C) = 3$ $\frac{COP_{HP}(T_{HP}^{in} = 50\,°C)}{COP_C(T_{HP}^{in} = 50\,°C)} = \frac{COP_{HP}(T_{HP}^{in} = 35\,°C)}{COP_C(T_{HP}^{in} = 35\,°C)}$ $COP_C = T_{HP}^{out} / (T_{HP}^{out} - T_{HP}^{in})$ $\dot{Q}_{HP}^{out,max}(T_{HP}^{in} = 50\,°C) = \dot{Q}_{HP}^{out,max}(T_{HP}^{in} = 35\,°C)$
HS	$\dot{En}_{HS}^{in} \cdot \eta_{HS} = \dot{Q}_{HS}^{out}$	$\eta_{HS} = \frac{\dot{Q}_{HS}^{out} / \theta_q(T = T_{HS}^{q,out})}{\dot{E}_{HS}^{in} / \theta_{ch}}$ $\theta_q(T = T_{HS}^{q,out}) = 1 - \frac{T_0}{T_{HS}^{q,out}}$ $(\theta_{ch} \approx 1 \;\; , \;\; T_0 = 8\,°C)$
DHN	$\dot{Q}_{DHN}^{in} = \dot{Q}_{DHN}^{out}$	$\dot{Q}_{HP}^{out} + \dot{Q}_{HS}^{out} = \dot{Q}_{DHN}^{in}$
SST	$\dot{Q}_{SST}^{in} = \dot{Q}_{SST}^{out}$	$\dot{Q}_{DHN}^{out} = \dot{Q}_{SST}^{in}$

Table A.2 compiles the concretized formulations of the exergy balance unit by unit. Further details about the energy and exergy models are available in the previous article [12]. The total exergy consumption by the LNCMI's processes is dissociated in 3 main terms: 1) "Useful" exergy destruction by the electromagnets ($\dot{E}_{LNCMI}^{D,use}$) in order to provide experimental data; 2) Recoverable outlet exergy in the form of waste heat ($\dot{E}_{LNCMI}^{out,q}$); 3) Exergy destruction ($\dot{E}_{LNCMI}^{D}$) mainly due to mechanical friction and heat losses. Only the third term was considered an irreversibility within LNCMI's

process. The temperature difference between the magnets and the waste heat ($\Delta T_{cooling}$) is constant and imposed by the magnets' cooling process [45].

Table A.2. Concretized formulation of the exergy balance for each unit.

Unit	Exergy balance	Auxiliary equations
LNCMI	$\dot{E}_{LNCMI}^{in} = \dot{E}_{LNCMI}^{D,use} + \dot{E}_{LNCMI}^{out,q} + \dot{E}_{LNCMI}^{D}$	$\dot{E}_{LNCMI}^{in} = \dot{W}_{LNCMI}^{in}$ $\dot{E}_{LNCMI}^{out,q} = \dot{W}_{LNCMI}^{in} \cdot \xi \cdot \theta_q(T = T_{LNCMI}^{out,q})$ $\dot{E}_{LNCMI}^{D,use} = \dot{W}_{LNCMI}^{in} \cdot \xi \cdot \left(\theta_{elec} - \theta_q(T = T_{LNCMI}^{magnets})\right)$ $T_{LNCMI}^{magnets} = T_{LNCMI}^{out,q} + \Delta T_{cooling}$
DISS	$\dot{E}_{DISS}^{D} = \dot{E}_{DISS}^{in,q}$	$\dot{E}_{LNCMI}^{out,q} = \dot{E}_{DISS}^{in,q} + \dot{E}_{TES}^{in,q}$
TES	$\dot{E}_{TES}^{in,q} = \dot{E}_{TES}^{out,q} + \Delta E_{TES}^{u} + \dot{E}_{TES}^{L}$	$\dot{E}_{TES}^{L} = \dot{Q}_{TES}^{L} \cdot \theta_q(T = T_{TES}^{in,q})$
HP	$\dot{E}_{HP}^{in,q} + \dot{W}_{HP}^{in} = \dot{E}_{HP}^{out,q} + \dot{E}_{HP}^{D}$	$\dot{E}_{HP}^{in,q} = \dot{Q}_{HP}^{in} \cdot \theta_q(T = T_{HP}^{in,q})$ $\dot{E}_{HP}^{out,q} = \dot{Q}_{HP}^{out} \cdot \theta_q(T = T_{HP}^{out,q})$
HS	$\dot{E}_{HS}^{in,ch} \cdot \varepsilon_{HS} = \dot{E}_{HS}^{out,q}$	$\varepsilon_{HS} = 0.4$ $\dot{E}_{HS}^{D} = \dot{Q}_{HS}^{out} \cdot \theta_q(T = T_{HS}^{q,out}) \cdot \left(\frac{1}{\varepsilon_{HS}} - 1\right)$
DHN	$\dot{E}_{HS}^{out,q} + \dot{E}_{HP}^{out,q} = \dot{E}_{DHN}^{out,q} + \dot{E}_{DHN}^{D}$	-
SST	$\dot{E}_{SST}^{in,q} = \dot{E}_{SST}^{out,q} + \dot{E}_{SST}^{D}$	$\dot{E}_{DHN}^{out,q} = \dot{E}_{SST}^{in,q}$

Table A.3 presents the concretized formulations of the cost flow balance unit by unit.

Table A.3. Concretized formulations of the cost flow balance unit by unit and their auxiliary equations.

Unit	Cost flow balance	Auxiliary equations
LNCMI	$\dot{C}_{LNCMI}^{D} = \dot{C}_{LNCMI}^{q,out}$	$c_{LNCMI}^{W,in} = c^{elec}$
DISS	$\dot{C}_{DISS}^{q,in} = \dot{C}_{DISS}^{D}$	$c_{DISS}^{q,in} = c_{LNCMI}^{q,out}$
TES	$c_{TES}^{q,in} + \dot{Z}_{TES} = c_{TES}^{q,out}$	$c_{TES}^{q,in} = c_{LNCMI}^{q,out}$
HP	$\dot{C}_{HP}^{q,in} + \dot{C}_{HP}^{elec,in} + \dot{Z}_{HP} = \dot{C}_{HP}^{q,out}$	$c_{HP}^{q,in} = c_{TES}^{q,out}$
HS	$\dot{C}_{HS}^{F} = \dot{C}_{HS}^{q,out}$	$c_{HS}^{F} = c_{SST}^{out,REF} \cdot \dot{E}_{SST,REF}^{q,out} / \dot{E}_{HS,REF}^{F,in}$ $c_{HS}^{q,out} = \left(c_{SST}^{q,in} \cdot \dot{E}_{SST,REF}^{in}\right) / \dot{E}_{HS,REF}^{q,out}$ $c_{HS}^{F} = \left(c_{HS}^{q,out} \cdot \dot{E}_{HS,REF}^{q,out}\right) / \dot{E}_{HS,REF}^{F}$
DHN	$\dot{C}_{HP}^{q,out} + \dot{C}_{HS}^{q,out} = \dot{C}_{DHN}^{q,out}$	-
SST	$\dot{C}_{SST}^{q,in} = \dot{C}_{SST}^{P,BEP}$	$c_{SST}^{q,in} = c_{DHN}^{q,out}$ $c_{SST}^{q,in} = \dot{C}_{SST,REF}^{q,out} / \dot{E}_{SST,REF}^{q,in}$

Appendix B. Extended results of the 4E model

Figure B.1 shows the energy-exergoeconomics and exergy-exergoeconomics analyses. The most promising designs are: {35 ˚C - 10 MWh to 40 MWh}, {50 ˚C, 40 MWh}, and {85 ˚C, 30 MWh to 40 MWh}. The {35 ˚C - 10 MWh} design is EXEC-optimal and the {85 °C - 40 MWh} design is ENER-optimal. Switching from EXEC-optimal to ENER-optimal passing through the Pareto-optimal solutions causes marginal increases in C_{GLOB}^{D} but marginal improvements in the *RACF* as a compensation.

Cases at 35 ˚C and from 10 MWh to 40 MWh are indisputable exergy-exergoeconomics Pareto-optimal solutions. The design with 10 MWh is EXEC-optimal as mentioned before, and the design with 40 MWh is EXER-optimal. The designs with 20 MWh or 30 MWh seem interesting as a compromise.

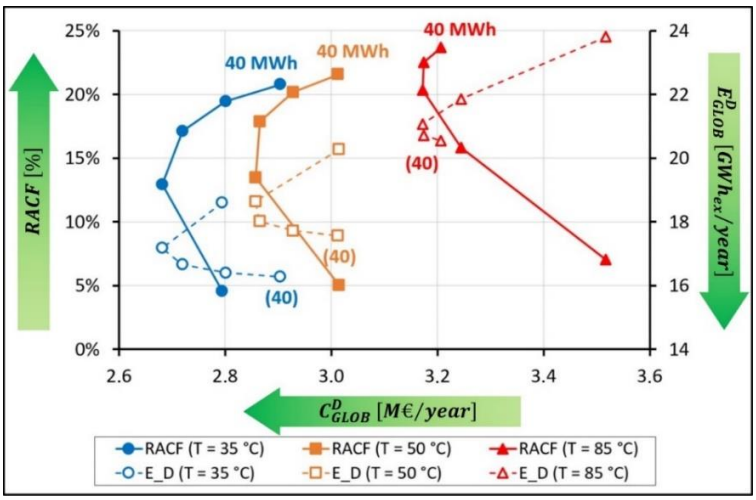

Figure B.1. Energy-exergoeconomics (*RACF* vs C^D_{GLOB}) and exergy-exergoeconomics Pareto fronts (E^D_{GLOB} vs C^D_{GLOB}) as function of storage capacity and inlet temperature.

Tables B.1 to B.8 show detailed results for each reference scenario, each monocriterion-optimal scenario and the multicriteria-optimal scenario. This study assessed two other well-known indicators, despite not using them as objective functions: the relative cost difference r (eq. A.1) and the exergoeconomic factor f (eq. A.2). The first expresses the increase in the average cost per exergy unit between fuel and product. The second defines the relative significance of the capital investment with respect to the total exergoeconomic expenses of the unit [11].

$$r = \frac{c^P - c^F}{c^F} \tag{A.1}$$

$$f = \frac{\dot{Z}}{\dot{Z} + \dot{C}^D} \tag{A.2}$$

Table B.1. Detailed metrics for the reference scenario at 35 °C (i.e. no waste heat recovery).

Parameter	LNCMI	DISS	TES	HP	HS	DHN	SST	GLOB	WHRS
Q^{in} $(GWh/year)$	0.0	18.4	-	-	0.0	23.5	23.5	41.9	-
W^{in} $(GWh/year)$	21.6	0.0	-	-	0.0	0.0	0.0	0.0	-
Q^{out} $(GWh/year)$	18.4	18.4	-	-	23.5	23.5	23.5	41.9	-
E^{in} $(GWh_{ex}/year)$	21.6	1.6	-	-	16.7	6.7	5.0	18.3	-
E^D $(GWh_{ex}/year)$	6.0	1.6	-	-	10.0	1.6	1.4	20.6	-
E^{out} $(GWh_{ex}/year)$	1.6	0.0	-	-	6.7	5.0	3.7	3.7	-
$\dot{C}^F$ $(k€/year)$	2596.8	267.3	-	-	1877.7	1877.7	1877.7	4474.5	-
$\dot{Z}$ $(k€/year)$	0.0	0.0	-	-	0.0	0.0	0.0	0.0	-
$\dot{C}^P$ $(k€/year)$	0.0	0.0	-	-	1877.7	1877.7	1877.7	1877.7	-
$\dot{C}^D$ $(k€/year)$	717.7	267.3	-	-	1126.6	460.6	514.5	3086.7	-
RR $(€/MWh_{th})$	0.0	0.0	-	-	80.0	0.0	0.0	80.0	-
f (%)	-	-	-	-	0	0	0	-	-
r (%)	-	-	-	-	0	0	0	-	-

Table B.2. Detailed metrics for the reference scenario at 50 °C (i.e. no waste heat recovery).

Parameter	LNCMI	DISS	TES	HP	HS	DHN	SST	GLOB	WHRS
Q^{in} $(GWh/year)$	0.0	18.4	-	-	0.0	23.5	23.5	41.9	-
W^{in} $(GWh/year)$	23.3	0.0	-	-	0.0	0.0	0.0	0.0	-
Q^{out} $(GWh/year)$	18.4	18.4	-	-	23.5	23.5	23.5	41.9	-
E^{in} $(GWh_{ex}/year)$	23.3	2.4	-	-	16.7	6.7	5.0	19.1	-
E^D $(GWh_{ex}/year)$	7.4	2.4	-	-	10.0	1.6	1.4	22.8	-
E^{out} $(GWh_{ex}/year)$	2.4	0.0	-	-	6.7	5.0	3.7	3.7	-
$\dot{C}^F$ $(k€/year)$	2791.6	420.0	-	-	1877.7	1877.7	1877.7	4669.2	-
$\dot{Z}$ $(k€/year)$	0.0	0.0	-	-	0.0	0.0	0.0	0.0	-
$\dot{C}^P$ $(k€/year)$	0.0	0.0	-	-	1877.7	1877.7	1877.7	1877.7	-
$\dot{C}^D$ $(k€/year)$	885.0	420.0	-	-	1126.6	460.6	514.5	3406.8	-
RR $(€/MWh_{th})$	0.0	0.0	-	-	80.0	0.0	0.0	80.0	-
f (%)	-	-	-	-	0	0	0	-	-
r (%)	-	-	-	-	0	0	0	-	-

Table B.3. Detailed metrics for the reference scenario at 85 °C (i.e. no waste heat recovery).

Parameter	LNCMI	DISS	TES	HP	HS	DHN	SST	GLOB	WHRS
Q^{in} $(GWh/year)$	0.0	18.4	0.0	0.0	0.0	23.5	23.5	41.9	0.0
W^{in} $(GWh/year)$	27.1	0.0	0.0	0.0	0.0	0.0	0.0	0.0	0.0
Q^{out} $(GWh/year)$	18.4	18.4	0.0	0.0	23.5	23.5	23.5	41.9	0.0
E^{in} $(GWh_{ex}/year)$	27.1	4.0	0.0	0.0	16.7	6.7	5.0	20.7	0.0
E^{D} $(GWh_{ex}/year)$	10.7	4.0	0.0	0.0	10.0	1.6	1.4	27.7	0.0
E^{out} $(GWh_{ex}/year)$	4.0	0.0	0.0	0.0	6.7	5.0	3.7	3.7	0.0
$\dot{C}^{F}$ $(k€/year)$	3246.0	786.5	0.0	0.0	1877.7	1877.7	1877.7	5123.7	0.0
$\dot{Z}$ $(k€/year)$	0.0	0.0	0.0	0.0	0.0	0.0	0.0	0.0	0.0
$\dot{C}^{P}$ $(k€/year)$	0.0	0.0	0.0	0.0	1877.7	1877.7	1877.7	1877.7	0.0
$\dot{C}^{D}$ $(k€/year)$	1287.3	786.5	0.0	0.0	1126.6	460.6	514.5	4175.5	0.0
RR $(€/MWh_{th})$	0.0	0.0	0.0	0.0	80.0	0.0	0.0	80.0	0.0
f (%)	-	-	0%	0%	0	0	0	-	0%
r (%)	-	-	0%	0%	0	0	0	-	0%

Table B.4. Detailed metrics for the {85 °C - 40 MWh} scenario (energy-optimal scenario).

Parameter	LNCMI	DISS	TES	HP	HS	DHN	SST	GLOB	WHRS
Q^{in} $(GWh/year)$	0.0	8.3	10.1	0.0	0.0	23.5	23.5	31.8	10.1
W^{in} $(GWh/year)$	27.1	0.0	0.0	0.0	0.0	0.0	0.0	0.0	0.0
Q^{out} $(GWh/year)$	18.4	8.3	10.1	0.0	13.4	23.5	23.5	31.7	0.0
E^{in} $(GWh_{ex}/year)$	27.1	1.8	2.2	0.0	9.5	3.8	5.0	11.3	2.2
E^{D} $(GWh_{ex}/year)$	10.7	1.8	0.0	0.0	5.7	0.9	1.4	20.5	0.0
E^{out} $(GWh_{ex}/year)$	4.0	0.0	2.2	0.0	3.8	5.0	3.7	3.7	2.2
$\dot{C}^{F}$ $(k€/year)$	3246.0	353.6	346.3	0.0	1070.1	2144.2	2144.2	4316.1	346.3
$\dot{Z}$ $(k€/year)$	0.0	0.0	586.9	54.4	0.0	0.0	0.0	641.3	641.3
$\dot{C}^{P}$ $(k€/year)$	346.3	0.0	933.2	54.4	1070.1	2144.2	2144.2	2144.2	987.6
$\dot{C}^{D}$ $(k€/year)$	1287.3	353.6	1.2	0.0	642.0	335.1	587.5	3206.8	1.2
RR $(€/MWh_{th})$	18.4	0.1	25.0	2.3	45.6	0.0	0.0	91.4	27.3
f (%)	-	-	100%	100%	0	0	0	-	100%
r (%)	-	-	136%	5%	0	0	0	-	185%

Table B.5. Detailed metrics for the {50 °C, 20 MWh} scenario (economy-optimal scenario).

Parameter	LNCMI	DISS	TES	HP	HS	DHN	SST	GLOB	WHRS
Q^{in} $(GWh/year)$	0.0	10.7	7.7	7.7	0.0	23.5	23.5	31.9	7.7
W^{in} $(GWh/year)$	23.3	0.0	0.0	2.3	0.0	0.0	0.0	2.3	2.3
Q^{out} $(GWh/year)$	18.4	10.7	7.7	10.0	13.5	23.5	23.5	34.2	10.0
E^{in} $(GWh_{ex}/year)$	23.3	1.4	1.0	3.3	9.6	6.0	5.0	14.3	4.3
E^{D} $(GWh_{ex}/year)$	7.4	1.4	0.0	1.2	5.8	0.9	1.4	18.0	1.2
E^{out} $(GWh_{ex}/year)$	2.4	0.0	1.0	2.2	3.8	5.0	3.7	3.7	3.2
$\dot{C}^{F}$ $(k€/year)$	2791.6	244.1	163.7	249.4	1076.6	1911.9	1911.9	3868.2	413.1
$\dot{Z}$ $(k€/year)$	0.0	0.0	293.5	85.8	0.0	0.0	0.0	379.2	379.2
$\dot{C}^{P}$ $(k€/year)$	163.7	0.0	457.1	335.2	1076.6	1911.9	1911.9	1911.9	792.3
$\dot{C}^{D}$ $(k€/year)$	885.0	244.1	0.6	265.3	646.0	300.4	523.8	2865.2	265.8
RR $(€/MWh_{th})$	7.5	0.3	12.5	15.6	45.9	0.0	0.0	81.8	28.1
f (%)	-	-	100%	24%	0	0	0	-	59%
r (%)	-	-	168%	72%	0	0	0	-	92%

Table B.6. Detailed metrics for the {35 °C, 40 MWh} scenario (exergy-optimal scenario).

Parameter	LNCMI	DISS	TES	HP	HS	DHN	SST	GLOB	WHRS
Q^{in} $(GWh/year)$	0.0	10.6	7.8	7.7	0.0	23.5	23.5	30.3	7.8
W^{in} $(GWh/year)$	21.6	0.0	0.0	3.8	0.0	0.0	0.0	3.8	3.8
Q^{out} $(GWh/year)$	18.4	10.6	7.7	11.5	11.9	23.5	23.5	34.1	11.5
E^{in} $(GWh_{ex}/year)$	21.6	0.9	0.7	4.5	8.5	5.9	5.0	13.9	5.2
E^{D} $(GWh_{ex}/year)$	6.0	0.9	0.0	2.0	5.1	0.8	1.4	16.3	2.0
E^{out} $(GWh_{ex}/year)$	1.6	0.0	0.7	2.5	3.4	5.0	3.7	3.7	3.2
$\dot{C}^{F}$ $(k€/year)$	2596.8	154.5	112.8	455.1	953.8	2247.6	2247.6	3550.6	567.9
$\dot{Z}$ $(k€/year)$	0.0	0.0	586.9	132.1	0.0	0.0	0.0	719.0	719.0
$\dot{C}^{P}$ $(k€/year)$	112.8	0.0	699.7	587.1	953.8	2247.6	2247.6	2247.6	1286.9
$\dot{C}^{D}$ $(k€/year)$	717.7	154.5	1.0	524.1	572.3	318.5	615.8	2903.9	525.1
RR $(€/MWh_{th})$	4.8	0.1	25.0	25.3	40.6	0.0	0.0	95.8	50.3
f (%)	-	-	100%	20%	0	0	0	-	58%
r (%)	-	-	526%	103%	0	0	0	-	127%

Table B.7. Detailed metrics for the {35 °C - 10 MWh} scenario (exergoeconomics-optimal scenario).

Parameter	LNCMI	DISS	TES	HP	HS	DHN	SST	GLOB	WHRS
Q^{in} $(GWh/year)$	0.0	12.3	6.1	6.1	0.0	23.5	23.5	32.7	6.1
W^{in} $(GWh/year)$	21.6	0.0	0.0	3.1	0.0	0.0	0.0	3.1	3.1
Q^{out} $(GWh/year)$	18.4	12.3	6.1	9.2	14.3	23.5	23.5	35.8	9.2
E^{in} $(GWh_{ex}/year)$	21.6	1.1	0.5	3.6	10.2	6.0	5.0	14.9	4.1
E^{D} $(GWh_{ex}/year)$	6.0	1.1	0.0	1.6	6.1	1.0	1.4	17.2	1.6
E^{out} $(GWh_{ex}/year)$	1.6	0.0	0.5	2.0	4.1	5.0	3.7	3.7	2.5
$\dot{C}^{F}$ $(k€/year)$	2596.8	178.4	88.8	235.7	1145.6	1879.3	1879.3	3742.4	324.5
$\dot{Z}$ $(k€/year)$	0.0	0.0	146.7	132.1	0.0	0.0	0.0	278.8	278.8
$\dot{C}^{P}$ $(k€/year)$	88.8	0.0	235.6	367.7	1145.6	1879.3	1879.3	1879.3	603.3
$\dot{C}^{D}$ $(k€/year)$	717.7	178.4	0.2	271.4	687.4	311.0	514.9	2681.1	271.6
RR $(€/MWh_{th})$	3.8	1.9	6.3	21.2	48.8	0.0	0.0	81.9	27.5
f (%)	-	-	100%	33%	0	0	0	-	51%
r (%)	-	-	166%	122%	0	0	0	-	86%

Table B.8. Detailed metrics for the {35 °C - 30 MWh} scenario (multicriteria-optimal scenario).

Parameter	LNCMI	DISS	TES	HP	HS	DHN	SST	GLOB	WHRS
Q^{in} $(GWh/year)$	0.0	10.9	7.5	7.5	0.0	23.5	23.5	30.7	7.5
W^{in} $(GWh/year)$	21.6	0.0	0.0	3.7	0.0	0.0	0.0	3.7	3.7
Q^{out} $(GWh/year)$	18.4	10.9	7.5	11.2	12.3	23.5	23.5	34.4	11.2
E^{in} $(GWh_{ex}/year)$	21.6	1.0	0.7	4.4	8.7	5.9	5.0	14.1	5.0
E^{D} $(GWh_{ex}/year)$	6.0	1.0	0.0	2.0	5.2	0.9	1.4	16.4	2.0
E^{out} $(GWh_{ex}/year)$	1.6	0.0	0.7	2.4	3.5	5.0	3.7	3.7	3.1
$\dot{C}^{F}$ $(k€/year)$	2596.8	158.2	109.0	390.5	982.7	2111.5	2111.5	3579.5	499.5
$\dot{Z}$ $(k€/year)$	0.0	0.0	440.2	132.1	0.0	0.0	0.0	572.3	572.3
$\dot{C}^{P}$ $(k€/year)$	109.0	0.0	549.2	522.5	982.7	2111.5	2111.5	2111.5	1071.8
$\dot{C}^{D}$ $(k€/year)$	717.7	158.2	0.7	449.7	589.6	307.0	578.5	2801.5	450.4
RR $(€/MWh_{th})$	4.6	0.1	18.8	24.7	41.9	0.0	0.0	90.1	43.4
f (%)	-	-	100%	23%	0	0	0	-	56%
r (%)	-	-	407%	106%	0	0	0	-	115%